BORONIC ACID CONJUGATED PEPTIDE AMPHIPHILE SYSTEMS FOR CONTROLLED DRUG RELEASE

A THESIS SUBMITTED TO

THE GRADUATE SCHOOL OF ENGINEERING AND SCIENCE

OF BILKENT UNIVERSITY

IN PARTIAL FULFILLMENT OF THE REQUIREMENTS FOR

THE DEGREE OF

MASTER OF SCIENCE

IN

MATERIALS SCIENCE AND NANOTECHNOLOGY

By

Hatice Kübra Kara

August 2017

BORONIC ACID CONJUGATED PEPTIDE AMPHIPHILE SYSTEMS FOR CONTROLLED DRUG RELEASE

By Hatice Kübra Kara

August 2017

We certify that we have read this thesis and that in our opinion it is fully adequate, in scope and in quality, as a thesis for the degree of Master of Science.

Eda Yılmaz (Advisor)

Mustafa Özgür Güler (Co-advisor)

Bilge Baytekin

Özgül Persil Çetinkol

Approved for the Graduate School of Engineering and Science:

Ezhan Karaşan
Director of the Graduate School

ABSTRACT

BORONIC ACID CONJUGATED PEPTIDE AMPHIPHILE SYSTEMS FOR THE CONTROLLED DRUG RELEASE

Hatice Kübra Kara
M.Sc. in Materials Science and Nanotechnology
Advisor: Eda Yılmaz
Co-advisor: Mustafa Özgür Güler
August 2017

Targeted cancer drug delivery is still under investigation and scientists have been focusing on major differences between healthy and cancer tissue to develop novel effective therapies. The cancer microenvironment has different physiological properties than the healthy tissues, for instance, it has more acidic pH, and much of the attention has been given to developing stimuli responsive agents for targeted drug delivery applications. Boronic acid is one of the most well-known stimuli responsive molecule which can form reversible covalent bonds with vicinal diols such as saccharide or catechol, that achieves targeted cancer drug release in a pH dependent manner. At neutral pH, the bond formation is triggered; however, these bonds become weaker at slightly acidic environment. Boronic acid conjugated polymers have been frequently preferred for doxorubicin encapsulation, which is a widely used chemotherapeutic drug utilized to treat several cancer types. In this study, boronic

acid and DOPA conjugated peptide amphiphiles were used as a biocompatible and biodegradable alternative to polymeric systems. Peptide amphiphiles self assemble to form peptide nanofibers via noncovalent interactions, such as hydrogen bonding, hydrophobic interactions, van der Waals forces and electrostatic interactions, where boronic acid/DOPA units remain on the exterior part of the nanofibers. In addition to noncovalent interactions, at physiological pH, boronic acid and DOPA moieties on the peptide surface form reversible covalent complexes, resulting in improved hydrogel strength, self-healing capacity and entrapment of doxorubicin inside the 3D-network. On the other hand, under acidic conditions, these interactions weaken and doxorubicin release is accelerated at tumor site. Reversible covalent interaction, secondary structure, morphological, mechanical, release profile analysis were performed on the system. Results showed that this system exhibits promising features that can be used for therapeutic applications.

Keywords: Peptide amphiphiles, self-assembly, boronic acid, hydrogels, controlled drug release, self-healing biomaterials, stimuli responsive systems

ÖZET

BORONİK ASİT KONJUGE EDİLMİŞ PEPTİT AMFİFİL SİSTEMLERİNİN KONTROLLÜ İLAÇ SALINIM UYGULAMASI

Hatice Kübra Kara
Malzeme Bilimi ve Nanoteknoloji Programı, Yüksek Lisans
Tez Danışmanı: Eda Yılmaz
Tez Eşdanışmanı: Mustafa Özgür Güler
Ağustos 2017

Hedeflenmiş kanser ilaç taşıma sistemleri halen araştırılmakta olup, bilim insanları, yeni etkili tedaviler geliştirmek için sağlıklı ve kanserli dokular arasındaki farklılıklara odaklanmaktadır. Kanser dokusu ortamı vücudun geri kalanından daha asidiktir; bu nedenle, uyarıya duyarlı maddeler, hedeflemeli ilaç taşıma uygulama sistemleri için büyük önem taşımaktadır. Boronik asit, sakkarit veya katekoller gibi diyollerle tersinir bağ kurabilen uyarıya duyarlı en popüler moleküllerden biridir. Bağ oluşumu nötr pH'ta tetiklenirken, bu bağlar hafif asidik ortamda zayıflar. En çok bilinen kemoterapik ilaçlardan biri olan doksorubisini kapsüle etmek için boronik asit ve diyol konjuge edilmiş polimerler sıklıkla kullanılır. Bu çalışmada biyolojik olarak uyumlu ve bozunabilir boronik asit ve DOPA‘ya konjuge edilmiş peptit amfifiller polimerik sistemlere alternatif olarak kullanılmıştır. Bu PA'lar, elektrostatik etkileşimler, hidrojen bağları, Van der Waals kuvvetleri ve hidrofobik etkileşimler gibi kovalent olmayan etkileşimler yoluyla kendiliğinden biraraya

gelerek peptit nanofiber yapısını oluştururlar ve oluşan bu yapının dış yüzeyinde boronik asit/DOPA molekülleri bulunur. Kovalent olmayan etkileşimlere ilaveten, nano fiber yüzeyinde bulunan boronik asit ve DOPA, fizyolojik pH'de tersinir kovalent kompleksler oluşturarak, hidrojel kuvvetini, hidrojelin kendi kendine iyileşme kapasitesini ve doksorubisinin jel içinde tutulmasını artırmaktadır. Bununla birlikte, asidik pH'de, bu etkileşimler zayıflar ve doksorubisin salımı tümör bölgesinde hızlanır. İkincil yapı, morfolojik ve mekanik analizler, ilaç salınım profilleri ve tersinir kovalent etkileşimler test edilmiştir. Elde ettiğimiz sonuçlar bu sistemin ileri uygulamalar için uygun olduğunu göstermektedir.

Anahtar kelimeler: Peptit amfifiller, kendiliğinden bir araya gelme, boronik asit, hidrojel, kontrollü ilaç salımı, kendi kendini iyileştiren biyomateryaller, uyarılara duyarlı sistemler

Acknowledgement

I would like to express my thanks to my MSc advisor Eda Yılmaz for her support throughout my graduate studies. I also thank to Mrs. Zeynep Erdoğan and other engineers for their technical contribution to my thesis. I also would like to thank Bilkent University and The Scientific and Technological Research Council of Turkey (TUBİTAK) for their financial support.

I would like to express my special thanks to my friends for their scientific knowledge, fruitful collaboration and friendship during my MSc and I believe that their endless support and friendship will continue throughout my life.

Contents

List Of Figures

Abbreviations

ARS	Alizarin Red-S
Boc	*Tert*-butoxycarbonyl
BTZ	Bortezomid
CD	Circular dichroism
DCM	Dichloromethane
DIEA	*N*,*N*-diisopropylethylamine
DMF	N,N-Dimethylformamide
Dox	Doxorubicin-HCl
ECM	Extracellular matrix
ESI	Electrospray ionization
Fmoc	9-Fluorenylmethoxycarbonyl
HBTU	*N*,*N*,*N*′,*N*′-Tetramethyl-O-(1*H*-benzotriazole-1-yl) uronium hexafluorophosphate
HPLC	High pressure liquid chromatography
LC-MS	Liquid chromatography-mass spectroscopy
L-DOPA	Levo-DOPA (L-3,4-dihydroxyphenylalanine)
Mtt	4-Methyltrityl
NMR	Nuclear magnetic resonance
PA	Peptide amphiphile
RGD	Arginylglycylaspartic acid
QTOF	Quadrapole time of flight
SEM	Standard error of mean
SEM	Scanning electron microscopy
TEM	Transmission electron microscopy
TFA	Trifluoroacetic acid
TIS	Triisopropyl silane
UV-VIS	Ultraviolet Visible

Chapter 1

Introduction

1.1 Self-Assembly:

Self-assembly is a spontaneous process, which induces molecules to form a more thermodynamically stable and a well-defined structure via noncovalent forces under equilibrium conditions. In nature, molecular self-assembly is a unique bottom up process to construct with different length scales of complex biological structure using different building blocks. Peptides, lipids, nucleic acids and saccharides that are used to build up lipid bilayer cell membrane, DNA double helix, protein folding, actin filaments and tobacco mosaic viruses (Figure 1.1) are well-known examples [1-7].

In the last centuries, scientists have utilized biomaterials by mimicking or being inspired by the natural organisms. Although noncovalent interactions consist of weak forces such as hydrogen bonding, π-π stacking, van der Waals, hydrophobic electrostatic interactions compared to covalent bonding, they have many advantages in different cases. For instance, they create systems which can self-adapt to

environmental changes, reprogram themselves for different stimulus and interactions. These interactions demonstrate reversible characteristics and show the ability to heal themselves under appropriate conditions. Moreover, they can form larger structures via supramolecular chemistry since self-assembly is an enthalpically and entropically driven process. In order to create large nanostructures via supramolecular chemistry, solution phase or lubricious surfaces are needed to obtain required mobility [2, 3, 8-10]. These nanostructures have been utilized in regenerative medicine, drug delivery, and also sensing systems [11].

1.2 Peptide and Their Self-Assemblies

Amino acids are the organic molecules, which play crucial roles in biological systems that contain amine and carboxyl functional groups with side chains. These side chains are specific to each amino acid and determine their chemical and physical properties. Amino acids are classified by their side chain properties such as charged (lysine, histidine, glutamic acid), polar uncharged (serine, asparagine), hydrophobic with an aliphatic (alanine, leucine, valine) or aromatic (tyrosine, phenylalanine)) side chain etc. [9-11].

Peptides are formed by the condensation of two amino acid via peptide bonds. In peptide bond formation, the carboxyl group of one amino acid reacts with the amine group of the other amino acid as shown in Figure 1.2. Furthermore, peptides can be composed of natural or synthetic amino acids that can form versatile self-assembled nanostructures by supramolecular chemistry. For instance, hydrophobic side chains are responsible for hydrophobic aggregations via π-π stacking and hydrophobic

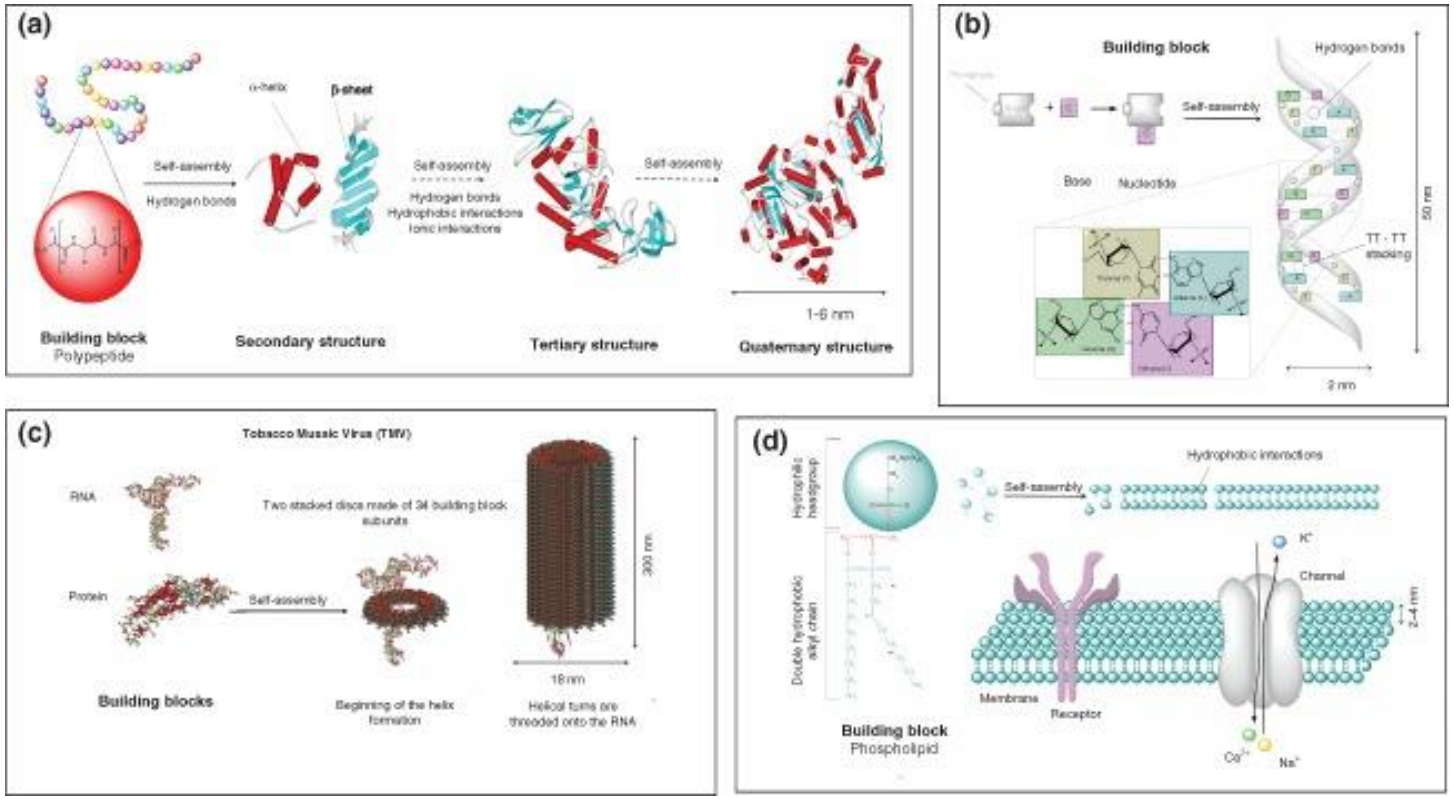

Figure 1.1 Examples of biological building blocks and their self-assembled structures . (a) Protein folding (b) ds-DNA (c) tobacco mosaic virus (d) cell membrane Reproduced from Ref. [4] with permission from John Wiley and Sons.

forces. In addition, polar amino acids utilize electrostatic forces or hydrogen bonding and peptide backbone itself promotes hydrogen bonds [12]. These hydrogen bonds result in constructing β-sheets conformation that stabilizes the multiple peptide arrangements. These sheets are further categorized as parallel and antiparallel β-sheets conformation according to the direction of the strands. Parallel conformation is obtained when the strands are placed in the same direction, while antiparallel β sheets are formed if the strands have opposite directions. Antiparallel conformation represents higher stability than parallel β-sheets since their pattern is more thermodynamically preferable. Furthermore, peptide strands can be arranged into right handed helix conformation by the repeating intramolecular hydrogen bonds between the amide groups and the carboxyl groups in same peptide with a pattern, *i,i+4*. In some instances, these structural α-helix motifs can produce different secondary structures by wrapping around each other, named coiled coil structures. The final secondary structure motif is the β-hairpin which is formed by having a short loop segment as a linker between two strands in antiparallel arrangement [12, 15-21]. Different secondary structural motifs of peptides self-assembly are demonstrated in Figure 1.3.

Peptides are biocompatible, biodegradable and bioactive in nature. Furthermore, self-assembly is a unique ability to fabricate a wide range of peptide nanostructures. Their architecture can be modified by changing the building blocks, amino acids, to obtain the desired functionality. Moreover, conjugation of peptides leads to increased diversity in peptides application fields [13]

In general, noncovalent interactions such as hydrogen bonding, hydrophobic, electrostatic and van der Waals forces, π–π stacking and coordination bonds are the

main interaction types, which govern the peptide self-assembly. The self-assembly events trigger bonds that form dynamic systems with the modulation of external factors such as pH, light, temperature, counterions, concentrations, and solvents [22-26].

pH is the most crucial external factor which effects the self-assembly of peptide by changing the charge of amino acid residues. Recently, pH change, triggering hydrogel formation has been paid attention for biomaterial studies.

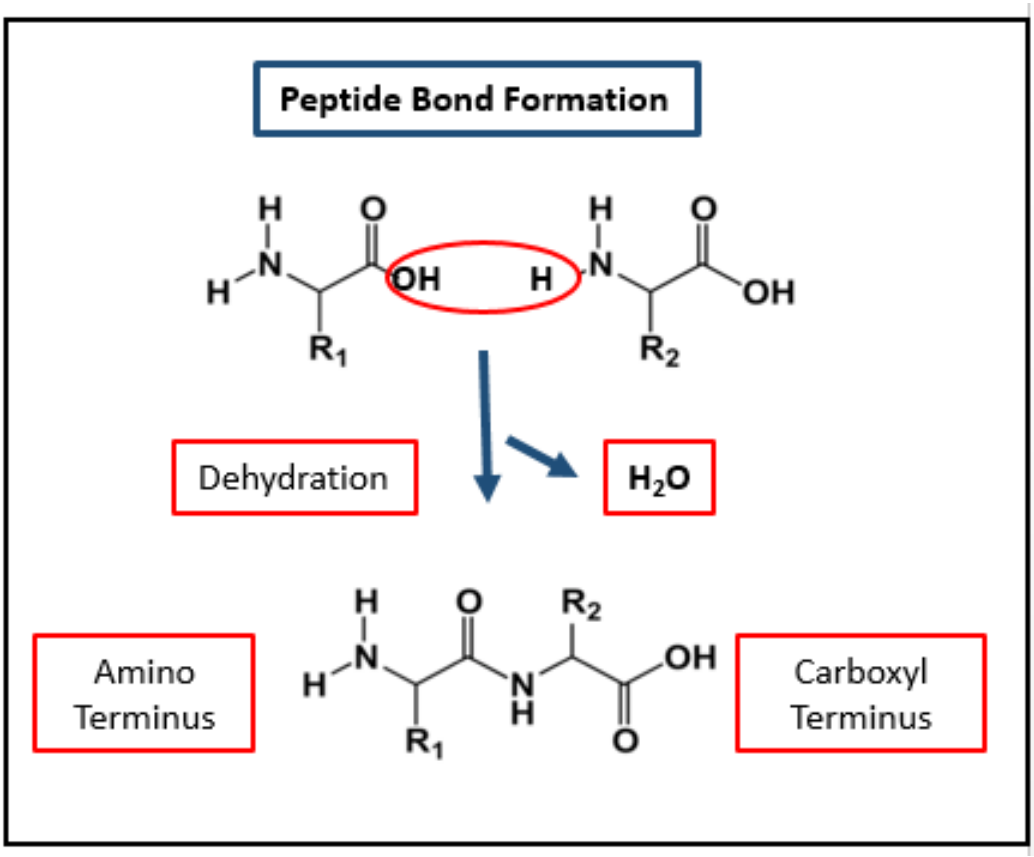

Figure 1.2 Peptide bond formation

Charged amino acid containing systems are neutralized by changing pH of the solution and a decrease in charge repulsion leads to an increase in inter/intra fiber

interaction. This results in aggregation and formation of different nanostructures. Furthermore, for charged amino acid containing peptide chains, pH change was also utilized in order to obtain controllable nanostructures [14-16]. For instance, Pandya et al. promoted the system that presented a parallel leucine zipper dimer under reducing conditions; however, when intramolecular disulfide bridge forms, it forms a monomeric helical hairpin architecture [17].

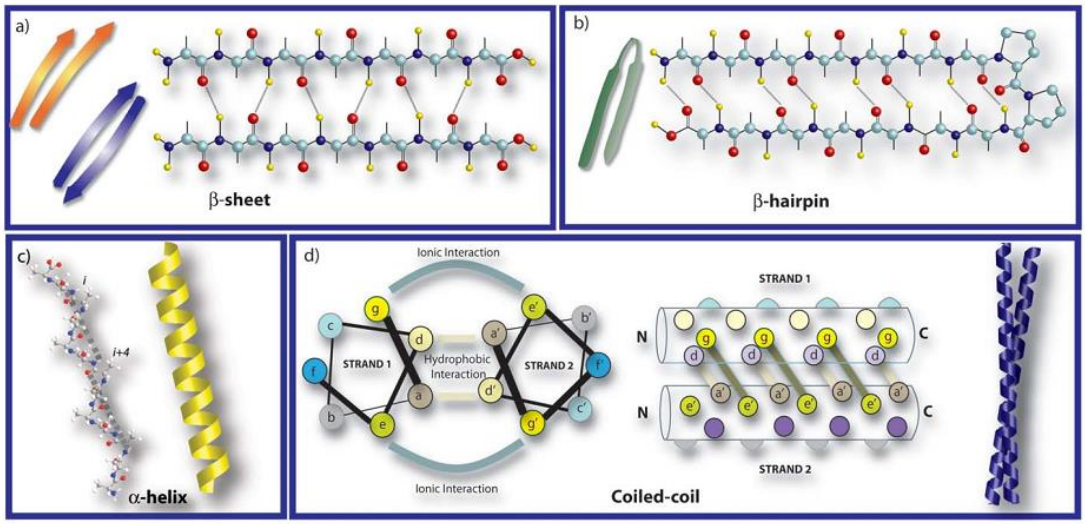

Figure 1.3 Schematic representation of different secondary structures of molecular self-assembly of peptides Adapted from Ref. [21] with permission from The Royal Society of Chemistry.

In addition to pH, effect of light on the self-assembly of peptide has also beem well investigated as well. For instance, Hilvert group claimed that photoinducible β-hairpins could be used for photo-control of peptide nanostructures. They synthesized meta-substituted azobenzene-containing peptides to form β-hairpins. When azobenzene derivative was in thermodynamically preferable trans form, structural

determination was not possible; however, after photo-isomerization linker turns into cis form, the structure was obtained as a β-hairpin [19].

Effects of temperature and solvent on peptide nanostructure were studied by Huang et al [20]. In their study, they offered temperature induced reversible diphenylalanine peptide self-assembling nanostructures. Applying external energy such as rising system temperature led to a change in nanostructures such as microtubes, nanowires or organogels in several solvents[20].

The salt concentration is another important factor for peptide self-assembly. In the literature, it is found that salt concentration has effects on nanostructures' kinetics of formation and architecture. Otsuka and their coworkers [22] studied peptide amphiphile sol-gel transition behavior at different concentration of sodium dihydrogenorthophosphate salt. They concluded that not only gelation speed and gel characteristics but also β-sheet content and nanostructure density were affected by salt concentrations [22].

These factors are the major external factors that influence the organization of peptide building blocks into different nanostructures; however, the control of the self-assembly of these nanostructures is still in progress. Therefore, investigation of the factors to build controllable peptide self-assemblies and tune their architectures is crucial.

1.3 Solid Phase Peptide Synthesis

Solid phase peptide synthesis (SPPS), which was firstly illustrated by Bruce Merrifield in 1963 [23], is the most suitable method for small to medium size peptide synthesis. This method shows superiority upon other techniques, since it enables fast,

simple and economical peptide synthesis, easy functional group coupling, high yields and stability under different conditions. In SPPS, solid support that is also called the resin is one of the most important factors because all peptide chains are constructed on this support. During the peptide synthesis, firstly, peptides are covalently bounded to the beads of resin followed by general coupling procedure. This is based on the repetition of following steps: deprotection of the amino acids-washing-coupling of the amino acid-washing (Figure 1.4). The amino acid, which is unprotected at the C-terminus and protected at the N-terminus are coupled with the unprotected N-terminus of amino acid on the solid support. After each step, in order to remove the remaining chemicals, the beads are washed and filtered followed by the addition of acetic anhydride to block the side reactions. After completion of the synthesis, the peptide is cleaved by the acidic reagent such as trifluoroacetic acid (TFA) which transfers peptide from solid support to solution phase.

1.4 Peptide Amphiphile

A chemical compound, which has both hydrophobic and hydrophilic properties, is called amphiphile and these kind of molecules are called amphiphilic or amphipathic molecules. Detergents, soaps and lipoproteins are the most common examples of amphiphile molecules. Peptide amphiphiles (PA) that are also known as lipidated peptides or lipopeptides are the one of the most well-known amphiphilic molecules existing in living organisms. These molecules consist of a lipid tail which is connected to a peptide and they can be described as peptide based compound that forms self-assembly structure. These amphiphilic molecules can take part in signal transduction pathway, defense mechanism of organisms and protein-protein or protein-lipid interactions [24-28].

Peptide amphiphiles are comprised of multidomains, these domains can be categorized into hydrophobic and hydrophilic parts. In 2000s, it was explained that peptide amphiphiles (Figure 1.5) are composed of 4 domains. First domain is a hydrophobic tail whose hydrophobicity is one of the most important major forces which triggers the self-assembly of PA into well-defined structures. Second domain is the β-sheet forming region, which typically comprises of short peptides constructing via hydrogen bonds. Third domain has charged residues to increase the water solubility and form self assembled nano-architecture via pH or salt effect. Both type and the number of the charged amino acids are necessary to obtain desired solubility and avoid the aggregation of PAs at physiological medium. The presence and the strength of these noncovalent interactions such as electrostatic forces, hydrogen bonding, hydrophobic interactions, π-π stacking determine the various morphologies of the PA nanostructure such as fibers, micelles, nanotapes, nanotubes, nanosheets (Figure 1.6) and these nanostructures gather to form 3D networks. Finally, bioactive epitope that decide the functionality of the nanostructure can be used for further applications [13, 18, 29-35]. Moreover, bioactive epitope has effects on physical, chemical and mechanical properties of 3D formed network [7, 13, 24, 36]. In the literature, PA containing biomaterials with various epitopes are utilized for several purposes such as adhesion, bioimaging and sensing etc. [7, 23, 29-32, 37].

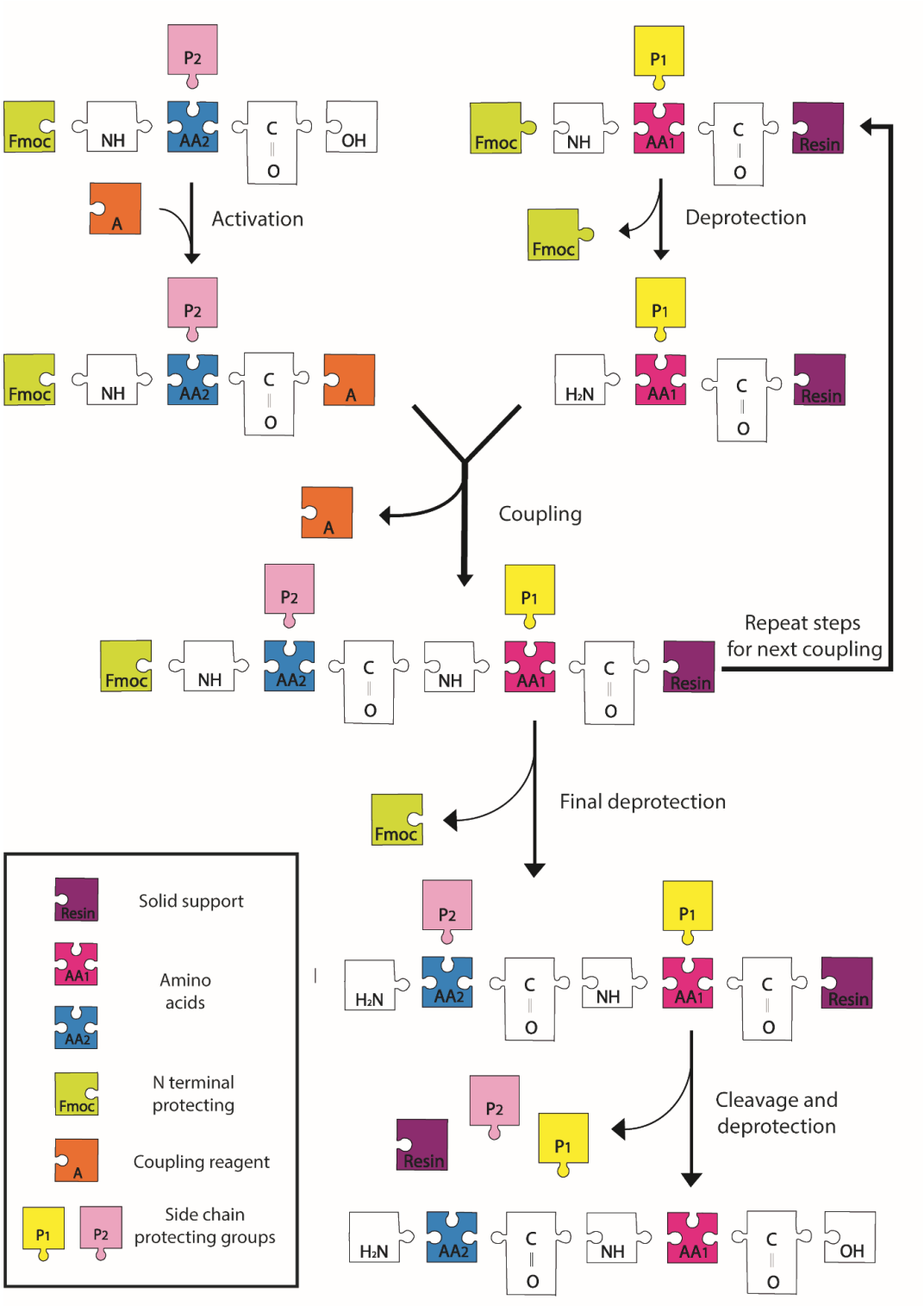

Figure 1.4 Schematic representation of Solid Phase Peptide Synthesis.

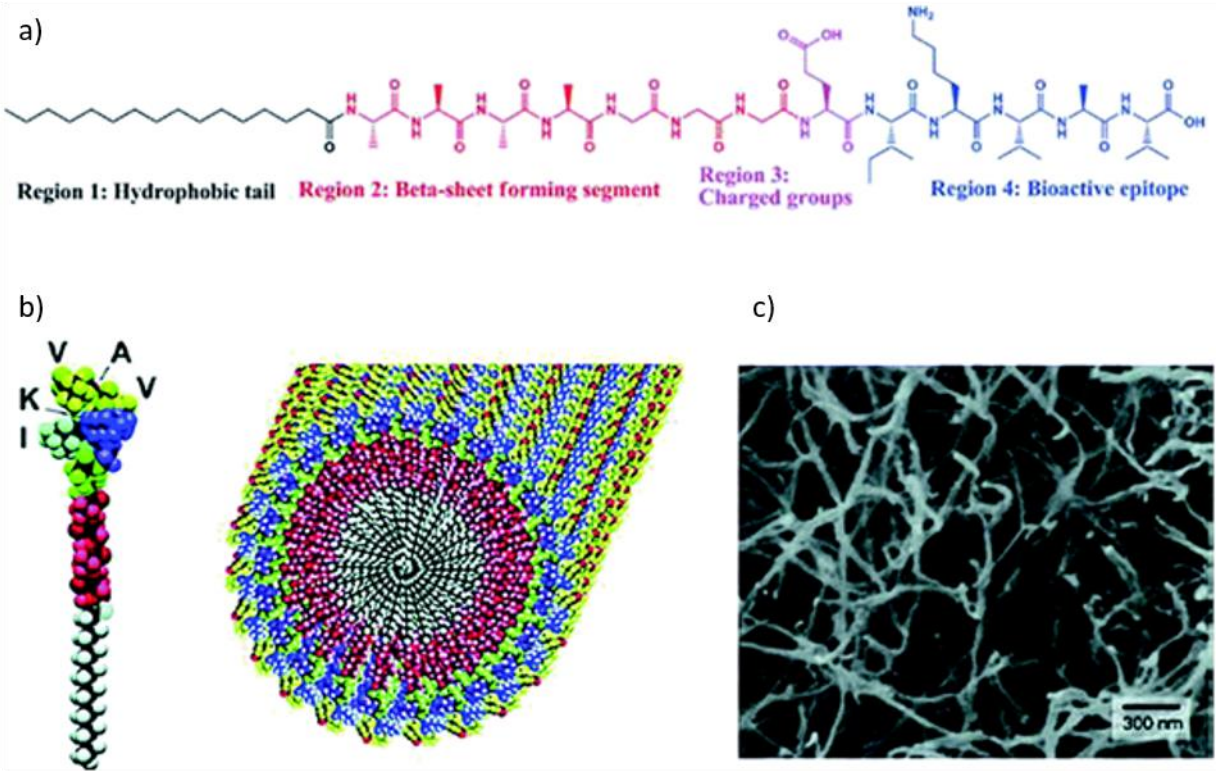

Figure 1.5 Schematic representation of self-assembly of PAs into nanofibers: a) Chemical structure of PA with four key chemical entities. b) Molecular model of an active epitope-containing PA, their self-assembly into nanofibers, as well as c) SEM image of nanofibers [35]

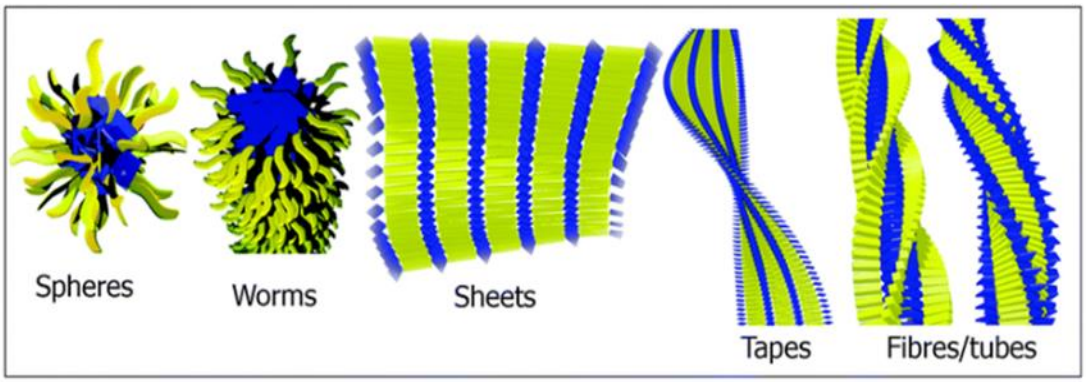

Figure 1.6 Peptide amphiphile self-assembly supramolecular nanostructures. Adapted from Ref. [18] with permission from The Royal Society of Chemistry.

1.5 Stimuli Responsive Peptide Systems

Stimuli responsive or smart/intelligent materials are unique systems which can modify themselves according to the environmental factors. These systems are sensitive to several external factors such as chemical, biological or physical stimuli (Figure 1.7) [38, 39].

Stimuli responsive biomaterials are used for different purposes such as diagnosis, imaging or sensing studies. Therefore, scientists have been developing several systems which can be liposomes, polymer nanoparticles, micelles, dendrimers, and inorganic nanoparticles made up of iron oxide, quantum dots, gold or metal oxide frameworks for a variety of biomedical and bionanotechnology applications [33].

Peptide based materials have been paid attention as stimuli responsive biomaterials due to their intrinsically bioactive, biocompatible, nontoxic and dynamic nature. In the literature, there are several stimuli responsive peptide containing systems designed for biotechnological applications such as drug delivery, tissue regeneration and sensing [13].

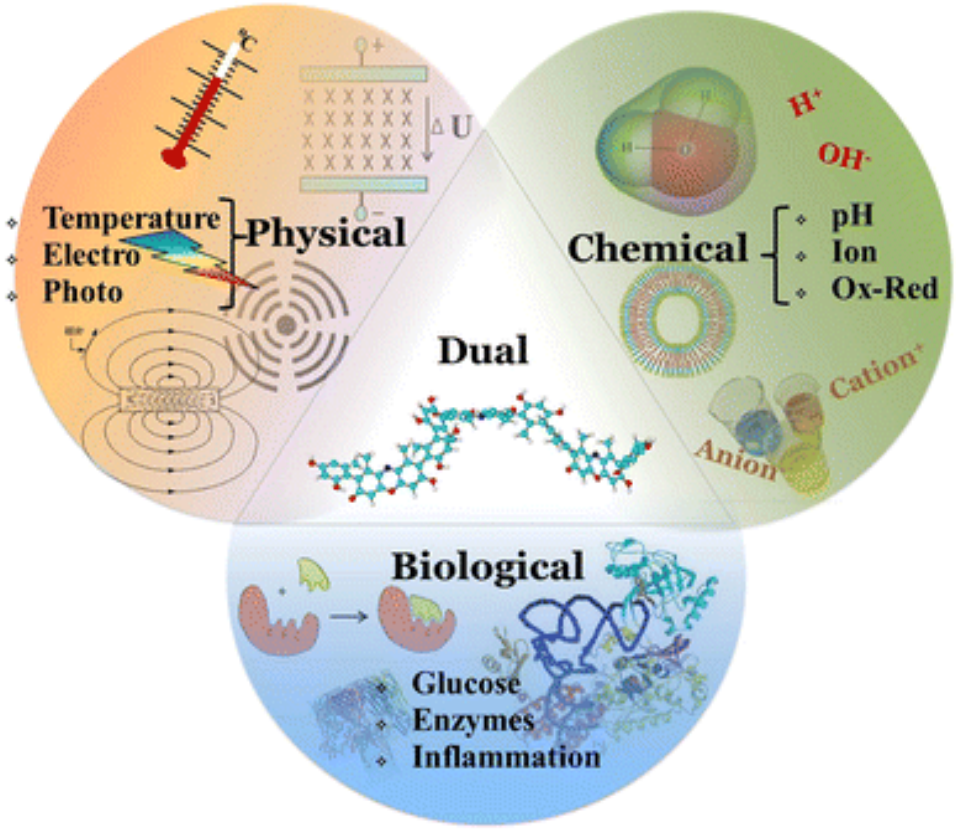

Figure 1.7 Categorization of physical, biological and chemical stimuli [39].

For instance, the Par-4 which is a pivotal protein for apoptotic pathways and C terminus of this protein is responsible for communicating with proposed effector molecules. The C terminus of Par-4 prefers to stay in monomeric form under physiological conditions; however, the coil coiled secondary structure is formed at low pH and temperature. It was reported that the native unfolded form of the C terminal residues affect the functions of cells and signaling pathways involved in several mechanisms. On the other hand, coil coiled structure is important in binding to effector molecules and forming complexes by the effect of external factors. These systems are effective for specific cancer types such as prostate cancer, various neurodegenerative disease such as Alzheimer's and Huntington's and HIV [40].

Furthermore, basic light triggered hydrogelation system was developed by Haines et al which [41] is the alternative of the toxic initiator materials. The 2 wt % solution of photocaged peptide MAX7CNB found in unfolded form in aqueous environment. The photocage was released after exposure to light between 260-360 nm and the peptides were self assembled into the β-hairpin structure which formed viscoelastic hydrogels. After *in vitro* analyses, it was proven that they possess nontoxic nature and allow adhesion and migration of the cells [41].

Moreover, Hartgerink et al synthesized pH responsive peptide amphiphile molecules that bear an integrin binding sequence RGD with different alkyl lengths [16]. The cysteine residue enables the system to form intramolecular crosslinks by disulfide bonds and a high molecular weight material is formed. They obtained the reversible nanostructure by changing the pH of the system which can be used for several biological and non-biological studies [16].

In another study, Beniash et al used peptide amphiphiles, with RGD sequence design that self assembled into 3D nanofibrillar networks by the aid of polyvalent and monovalent metal ions, which are incubated inside body fluid [42]. Changing the metal concentrations in the solution triggers the gelation of the system. During the gelation process, addition of cells to the solvent leads to the entrapment of cells inside the 3D matrix. This network enables the cell movement and proliferation during entrapment period and the survival of cells did not change for 3 weeks. This biomaterial has a potential to be used in regenerative medicine and cell transplantation studies.

Furthermore, Hartgerink et al studied biomineralization by pH induced self-assembly of PAs, where biomimicking biomaterials formed a fibrillar scaffold by reversible crosslinks at a specific pH range [34]. The thiols formed disulfides by oxidation and reverse reaction occured by the reduction of sulfide bond. In their study, suitable environment for direct hydroxyapatite mineralization was created, resulting in aligned composite materials which were similar to bone structure that has collagen fibrils and hydroxyapatite crystals.

Moreover, in another study, Jones et al used peptide conjugation with boronic acid that intrinsically had characteristic pH stimuli responsive features [43]. This system formed a nanoribbon above pH 5.5. Salt addition triggered the self-assembly of FF-boronic acid monomer and desired solubility was achieved by boronic acid group. Furthermore, this assembly is disturbed by polyol addition since boronic acid and catechol forms a boronate complex and the gel structure turns into a homogeneous solution. This material can be a suitable candidate for therapeutics and drug delivery applications.

Another example of a pH based structural transformation was presented by Gologan group [44]. They used heptane bolaamphiphile building blocks to design a stimuli responsive biomaterial. At pH 8, these building blocks formed a helical ribbon conformation; however, at acidic pH, they had tendency to build crystalline tubules. The conversion from helical ribbons to tubules happened in one day; however, reverse transformation happened more slowly [44]. This material can be improved for controlled release studies. In another study, Yang et al designed hydrogelator Nap-FFGEY which forms a supramolecular hydrogel [45]. The hydrogel formation was controlled by a switch between kinase/phosphatase to manage the

phosphorylation and dephosphorylation of the peptide. They used liquid form of hydrogelator for subcutaneous injection and observed the hydrogel formation at injected area. This material is a possible candidate for future applications in *in vivo* models of bioengineering studies. In another study, Zhang et al used dipeptide as a hydrogelator which responded to ligand receptor interactions and showed chiral detection [46]. This kind of specific ligand receptor interactions can be a unique ability to designing hydrogels for biosensing applications [46].

1.6 Boronic Acid

Boronic acid, a member of organoboranes, is an alkyl or aryl substituted boric acid and it is. It has one alkyl substituent and two hydroxyl groups to satisfy the valence shells on the boron atom. In neutral form, it has sp^2 hybridization and it has an empty p-orbital. This hybridization leads to obtain a trigonal planar geometry. Boronic acid can be obtained as secondary oxidation products of boranes. Their stability is higher than the first oxidation product, which is borinic acid and comparably less than third oxidation product that is boric acid. Boronic acid has several unique properties, which make it a desirable molecule for different purposes [47, 48].

Boronic acids are utilized as an intermediate and building block for important chemical synthesis reactions such as Suzuki coupling. It acts as a mild Lewis acid, which can accept lone pair electrons so it can react with strong Lewis bases such as fluoride, cyanide or phosphate anions. These properties make the boronic acid suitable material for homogeneous/heterogeneous and bulk/surface material sensing applications. Another unique ability of boronic acid is to form boronate ester via reversible covalent bonds with 1,2 or 1,3 cis-diols. It is a synthetic material that is

commonly used in biomedical and biotechnological applications due to being environmental friendly, its stability and biodegradability. The most extensively studied biological molecules reacting with boronic acid are saccharides, polysaccharides, nucleic acids, neurotransmitter dopamin and its derivative L-DOPA (Figure 1.8) [49]. The interactions of boronic acid with these molecules are used for detection, signaling pathway identification, enzyme inhibition, purification and cell/gene/drug delivery [47-52].

Although the exact reaction mechanism of boronate ester formation is not completely identified, formation of boronate ester from boronic acid and diol containing ligands are summarized in Figure 1.9 [53].

The boronic acid and their corresponding boronate ester represent sp^2 hybridization and trigonal planar electron domain geometry in neutral form (Figure 1.9a) and tetrahedral electron domain geometry and sp^3 hybridization in anionic form (Figure 1.9b). The reaction product between neutral and conjugate base of boronic acid with diol (Figure 1.9c,d) and the thermodynamically preferred structure of the boronic acid or the boronate ester are determined by the pKa value of the boronic acid or the boronate ester. In sp^2 hybridization, boron has an empty p orbital and the presence of Lewis bases leads to the production of anion in aqueous media. The pKa value of boronic acid conjugated systems changes between 4.5-10 depending on the substitution of the molecules. For biomedical applications, phenylboronic acid is widely used since phenyl group enables easy modification for the adjustment of pKa of the molecule [48, 51, 54].

The reaction tendency is controlled by the environment of the boronic acid such as pH, heat, solvent type, electric field, light and the analyte concentration and in addition to the substitutions of both boronic and ligand molecules. Although all these factors affect the boronic acid affinity, pH of the media and the substitution of the boronic acid are the most investigated parameters in the literature. Since boronate formation is only possible at specific pH range which is determined by the pKa values of the species, these values can be adjusted by the conjugation of boronic acid and diols. The diol/boronic acid reaction pH range has been studied to understand the

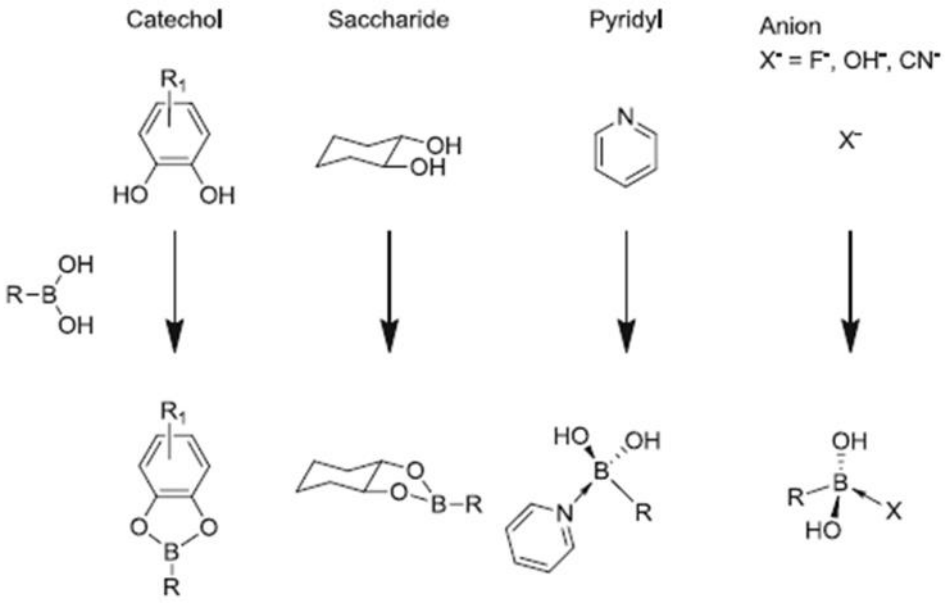

Figure 1.8 Boronic acid and its reaction with different molecules. Reproduced from Ref. [49] with permission from Springer.

exact interval. Different studies analyzed the suitable pH interval of boronic acid (R-$B(OH)_2$) and diol (H_2L) interactions under two different conditions. First, if

$pKa_{(R\text{-}B(OH)2)} \ll pKa_{(H2L)}$, suitable range can be identified as a $pKa_{(R\text{-}B(OH)2)} < pH < pKa_{(H2L)}$. On the other hand, if $pKa_{(R\text{-}B(OH)2)} >> pKa_{(H2L)}$, the crosslink formation is allowed at $pH = pKa_{R\text{-}B(OH)2} \pm 1$ [54, 55]. There are several diol molecules which can react with boronic acid; however, saccharides, L-DOPA and Alizarin Red are the most commonly used ones as diol containing molecules for different purposes [49, 55-58]. Their properties, interaction with boronic acid and applications will be explained later in detail in further sections.

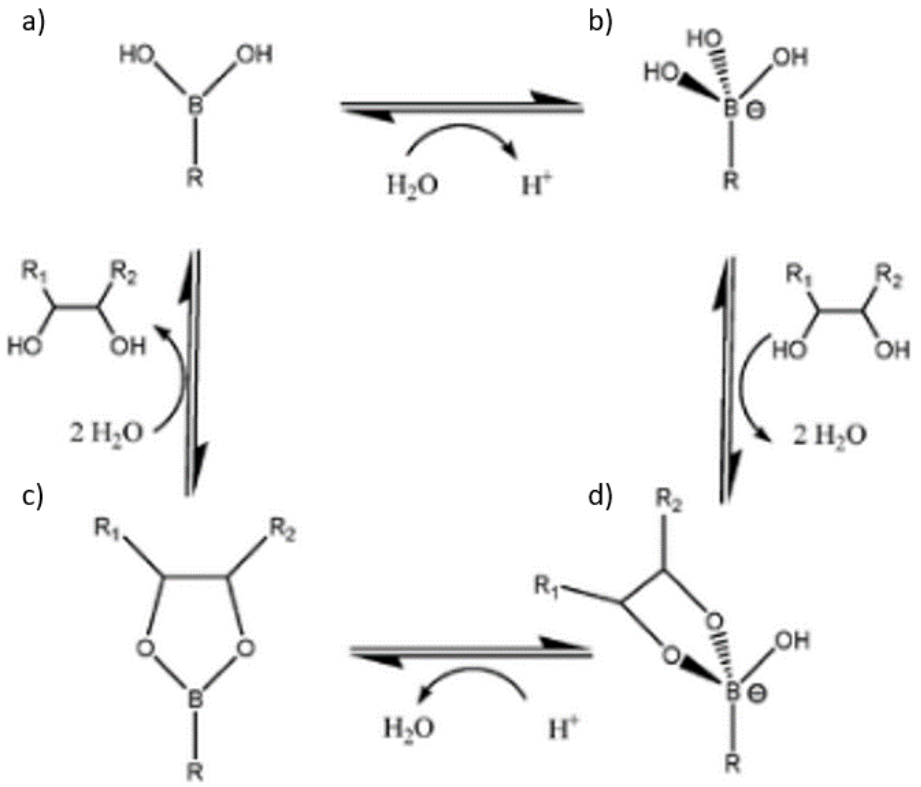

Figure 1.9 Multiple reaction mechanism of boronic acid. Reproduced from Ref. [51] with permission from The Royal Society of Chemistry.

1.6.1 Saccharides

One of the most abundant biological molecules inside the body are the saccharides that play crucial roles in events such as cell adhesion, immune response, bacterial invasion and tumor metastasis. However, by noncovalent interactions, it is hard to achieve high efficient sugar sensing. Another challenge for sugar sensing is the selectivity. Although they have different configurations of stereocenters, they represent similar chemical structures so earlier sensors slog on distinguishing saccharide and their immediate sensing. To overcome these problems, new and unique enzyme or lectin (sugar binding proteins) inspired synthetic chemosensor systems have been designed, which have superiority to the biological sensors in terms of stability under biological conditions and cost effectiveness. Therefore, boronic acid containing systems are unique and crucial chemosensors that have been utilized as saccharide sensors. It forms five- or six-membered cyclic esters with saccharides. They can achieve sensing at low concentrations at sub-milimolar levels. However, the most important property of boronic acid that makes it unique for sugar binding is that boronic acid can distinguish the orientation and relative position of hydroxyl groups of sugar and show selective affinity towards different saccharides. For instance, boronic acid has higher affinity toward fructose among monosaccharides when it is in monoboronic form. For phenyl boronic acid, the affinity order is fructose > galactose > mannose > glucose among monosaccharides. However, boronic acid and sugar in different forms such as polymer and self assembled systems exhibit different affinities and due to multivalency they demonstrate higher affinity, which will be, exemplified on section 1.7 [49, 53, 59-64].

1.6.2 Alizarin Red-S

Alizarin Red-S (ARS) which is a well-known catechol dye can react with boronic acid. This reaction leads to change in fluorescence activity of ARS and solution color. Thus, ARS and boronic acid interaction can be applicable for the concentration detection of boronic acid, recognition of competitive binding of other diol containing molecules and analyzing the affinity of boronic acid towards various molecules, both quantitatively and qualitatively. This assay is based on the transition between fluorescence active compound formation with ARS and its displacement with the competitive diol (Figure 1.10) [50, 52, 57, 65-68]. ARS and boronic acid are both fluorescence inactive; however, their boronate ester complex exhibit fluorescent property. Moreover, boronic acid, ARS and their mixtures possess different colors. Therefore, the formation of boronate ester between boronic acid/ARS and the replacement of ARS with a diol can be monitored by the change in color and using the fluorescence spectroscopy. In general, boronic acid and diol interactions can be achieved at neutral to slightly alkali medium with highly strong covalent bond characteristics. However, ARS can also bind to boronic acid at slightly acidic medium. ARS/Boronic acid complex can be destroyed with the addition of molecules which can bind to boronic acid by displacing ARS. Conclusively, formation of boronic acid/ARS complex leads to an increase in fluorescence intensity of the solution. Fluorescence intensity will decrease when a diol that has higher affinity to boronic acid than ARS is introduced to ARS/boronic acid solution. As a result, ARS based fluorescence assay is a unique method for detecting boronate ester formation. This assay makes the identification of boronic acid and target compounds interaction possible for different systems [50, 52, 54, 65-69].

These fluorescence based detection system can be explained by two separate spectra. Firstly, the boronic acid and ARS interactions needs to be examined to understand their dual behavior. At constant boronic acid concentration, increasing ARS amount leads to an increase in fluorescence signal. For the triple component system, another diol containing molecule is introduced into the system. If the molecule has a higher affinity towards boronic acid, the fluorescence active complex (boronic acid/ARS) will dissociate due to the replacement of ARS by the diol. In the literature, this method is utilized generally for the detection of free boronic acid, bond formation and binding constants [50, 66-68].

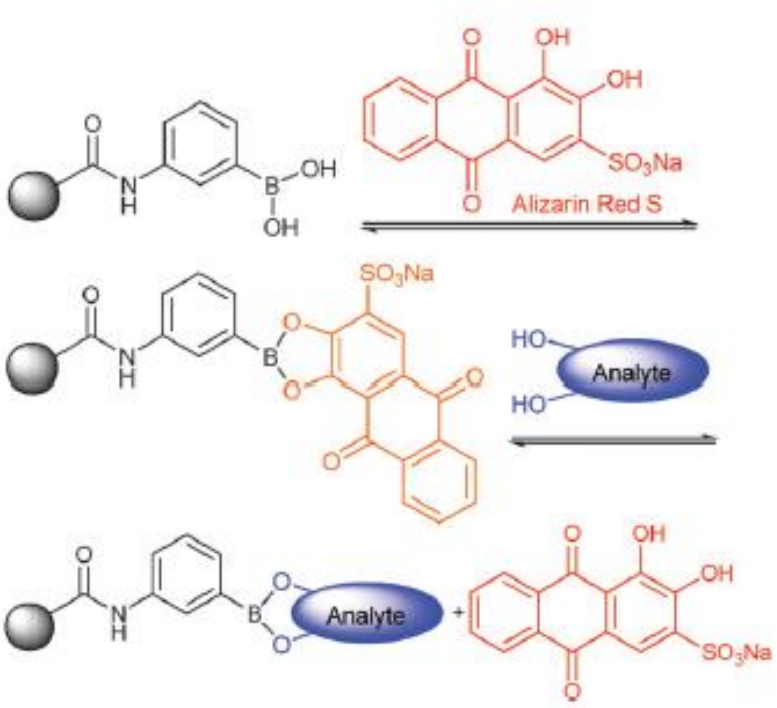

Figure 1.10 Binding and analyte-mediated release of Alizarin Red-S with hydrogel-bound boronic acid. Adapted from Ref. [65] with permission from The Royal Society of Chemistry.

Furthermore, UV-VIS spectroscopy is another tool for the detection of boronic acid using ARS dye. Boronic acid does not absorb in the UV-Vis region; while, ARS and ARS/boronic acid complex do absorb in UV-Vis region. Addition of boronic acid into the ARS solution leads to blue shift due to formation of boronic acid/ARS complex in the solution. On the contrary, destruction of this complex by adding other diols results in red shift [66].

1.6.3 L-DOPA

L-DOPA (Levo-DOPA) amino acid 3,4-dihydroxyphenylalanine (Figure 1.11) is a valuable molecule which has a wide range of potential applications. L-DOPA, that is called natural glue, is found in the secretion of mussels and responsible for adhesion. Nontoxic nature, quick adhesion process, high resistance to harsh conditions and stability in aqueous environment are the properties of this glue. Furthermore, wide range of temperatures and saline concentrations cannot interfere with adhesion and adhesion can be possible on several surfaces such as wood, metal and glass. However, L-DOPA loses its adhesion ability at a pH triggered by oxidation as opposed to reducing conditions. These properties make L-DOPA a suitable candidate for biomedical and biotechnological applications. Scientists have used the L-DOPA conjugated biomaterials as scaffolds, sensors, or surface coating materials. Its crosslink formation towards the surface are affected by the environmental conditions such as pH, antioxidant and electron withdrawing group functionalization which enables us to precisely control the adhesion [70-75].

In addition to its adhesion ability, DOPA plays an important role for neural system in the body. L-DOPA is a member of class that is called neurohormones like dopamine,

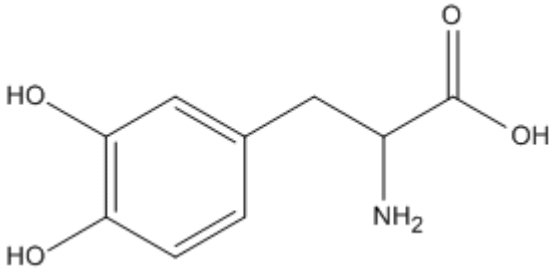

Figure 1.11 The chemical structure of L-DOPA

noradrenaline, L-tyrosine. Inside the body, there is a chain conversion between these molecules for instance, L-tyrosine is the precursor of L-DOPA, L-DOPA is converted into dopamine, and dopamine is the precursor of norepinephrine and epinephrine. All these molecules play a vital role for vital reaction inside the body such as heart rate/blood pressure adjustment and Parkinson's disease/hypertension/schizophrenia treatment. For instance decreasing the level of dopamine in the central nervous system can lead to Parkinson's disease; however, L-DOPA is used as a Parkinson drug. Although dopamine itself cannot penetrate through the blood-brain barrier, its precursor L-DOPA can pass through the blood-brain barrier and it is converted into dopamine in the brain. L-DOPA, Dopamine, epinephrine noradrenalin and DOPA-P, all have the catechol functional groups which can form a crosslinked structure with boronic acid. The formation of crosslinked structure can be used for real time *in vivo* molecule sensing, concentration determination and drug delivery. Similar to saccharide sensing, boronic acid have different affinities toward the catechol containing molecules. For instance, noradrenaline ≥ dopamine ≈ L-DOPA > catechol > DOPA-P is the order of affinity towards phenyl boronic acid; however, this order can be changed by the substitution of boronic acid or analyte molecules [70, 76-78].

1.7 Application Of Boronic Acid

The key point of boronic acid containing systems for biomedical applications is that it is controllable and forms strong reversible crosslinks with diols which is commonly found in biological molecules. The ability to form reversible and spontaneous interactions, biocompatibility and nontoxic nature are the desired properties of synthetic chemical systems for sensing, diagnostic and proteomics studies which is summarized in Figure 1.12 [50, 64, 79, 80]. However, single molecule systems are feeble, easy to break, and sometimes hard to detect. On the other hand, multivalent systems are much stronger and lean on each other. These systems exhibit superiority about the binding interactions, activity and availability. Therefore, multivalent systems of boronic acid can be used to prepare nano, micro and bulk architectures by using bottom up approach via the self-assembly or polymeric systems for various purposes [53].

In the literature, boronic acid conjugated polymer systems are frequently used as self-healing biomaterials due to their stimuli response and high self recovery capability [79-81]. For instance, boronic acid or diol containing PEG based hydrogel networks were utilized by the aid of boronate ester formation. PEG based mechanically controllable hydrogels that demonstrated high self-healing properties at neutral pH were obtained by Anderson group [79]. The rapid structural recovery was tested by rheological analysis and physical deformation, 100% recovery were exhibited by the reversible covalent bonds between cis-diol and boronic acid moieties [79]. This system showed highly suitable characteristics for tissue engineering as a 3D matrix or drug encapsulation network for the controlled drug release. This kind of examples can be multiplied under physiological conditions with

different building blocks and bioactive epitopes. However, at acidic pH the maintenance of self-healing properties of boronic acid containing systems is still problematic.

Sumerlin group published a study that achieved similar self-healing property at acidic pH [82]. They used an intramolecular coordination between boron in 2-acrylamidophenylboronic acid and the carbonyl oxygen that increase the stability of boronate ester structure. They used dopamine acrylamide copolymer and polyvinyl alcohol as diol containing groups. These interactions widen the pH range of the self-healing interval of hydrogels from neutral to acidic environment. The recovery ability of the hydrogels was tested by physically cutting the gel into two pieces. Then, the pieces were put together in contact and almost 1 h later they returned to the original appearance and no scar was observed. Moreover, rheological analyses were also used to understand the self-healing capacity and results demonstrated that both at acidic and neutral pH, hydrogels showed high self-recovery behavior.

Beside this, boronic acid conjugated systems have been recently used for controlled drug release or targeted drug delivery. Briefly, drug delivery systems have been improved to keep the drug release in desired level, sustain desired drug concentration at desired location, decrease side effects of toxic chemicals, and enhance bioavailability [83].

For biomedical and biotechnological applications, biodegradable, biocompatible, nontoxic, multifunctional, shape/size controlled intelligent drug delivery and controlled drug release systems have been developed [48, 50].

Boronic acid which is a smart molecule for the controlled drug release systems due to its intrinsic dynamic nature, controllable swelling property and tunable chemical interactions has been widely utilized [84]. Previously, boronic acid based systems were used for controlled insulin release according to glucose level. Kataoka et al [85] investigated smart insulin release system by utilizing P(NIPAM-co-3-AAPBA) hydrogels. This gel system formed a surface barrier layer in the deficiency of glucose and the insulin was encapsulated inside the gel matrix. However, increasing glucose concentration disrupted the layer and insulin can be released from the matrix.

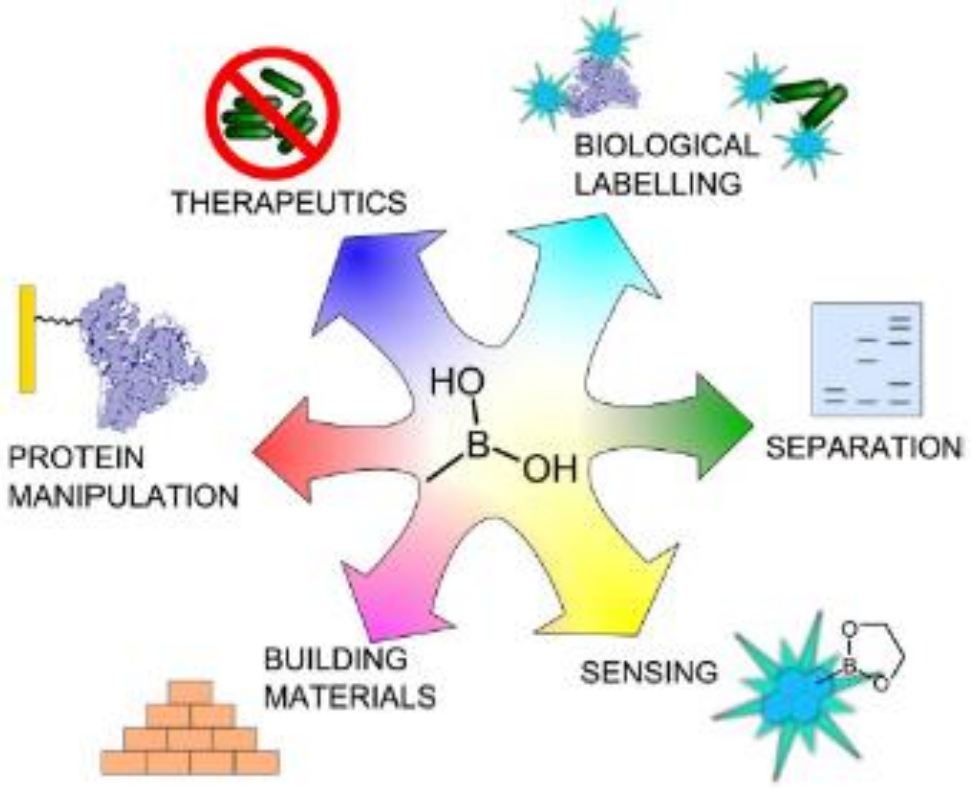

Figure 1.12 Several applications of boronic acid biomaterials [80].

As a result, glucose sensitive on-off release system was designed for self-regulated insulin release. In another study, nearly monodispersed microgels decorated with 3-aminophenylboronic acid were synthesized by Zhang et al [86]. Presence of glucose

leads to an increase in mesh size in alkali solution at room temperature because the stability of phenyl boronate ions were supported by the glucose/boronic acid complex and the release was accelerated [86].

Unlikely, in order to design glucose-responsive insulin-delivery system, Siddiqui group [87] proposed the system to increase glucose selectivity rather than fructose, which shows higher affinity towards boronic acid. 2-formyl-3- thienylboronic acid (FTBA) and 4-formylphenylboronic acid (FPBA) decorated chitosan nanoparticles were synthesized and the results showed that FTBA represented relatively higher affinity towards glucose and 1:1 ratio of boronic acid:chitosan showed higher glucose selectivity which can be used as a glucose responsive system that has a possible usage for insulin release under physiological conditions [87]. Furthermore, boronic acid has been used for cancer drug delivery systems. Cancer environment has slightly acidic medium than the physiological pH and boronic acid represented pH based stimuli responsive behavior. Therefore, boronic acid materials have been frequently used for cancer drug delivery [50]. For instance, dual responsive boronic acid and catechol conjugated crosslinked micelles have been demonstrated by Lam's group [50]. The polymers with boronic acid and catechol built self-assembling structures and intramolecular in situ bond formation of boronic acid/catechol was obtained. Then, drug got encapsulated inside the micelles at physiological pH, where boronate ester crosslink were preferred. However, release of drug accelerated at acidic pH or presence of compete diols due to weakening of the boronic acid-catechol bonds. Therefore, the nanoparticles maintained drug encapsulation in blood circulation; nevertheless, release can be possible at tumor microenvironment that possesses a more acidic ECM. Another example of pH and ligand concentration

triggered selective binding was studied on MCF-7 cancer cells by Liu et al [88]. Cells have the glycoproteins on the cell surfaces and by the sialic acid moieties cells can form a reversible bonds with grafted 3-APBA. At pH 6.8, boronic acid had higher tendency to bind sialic acid onto cell surface, which is the approximate pH value of the cancer microenvironment. Furthermore, existence of glucose blocked the sialic acid/boronic acid complexation because boronic acid prefers to bind glucose than sialic acid at physiologic pH. Therefore, the bond between cell and 3-APBA formed at lower pH were released reversibly at higher pH and glucose concentration.

Beside drug delivery systems, there is a boronic acid containing drug called Bortezomid (BTZ) (Figure 1.13) which is used as a proteasome inhibitor [89, 90]. It is composed of N-protected dipeptide with boronic acid that is placed on the C-terminus instead of the carboxylic acid.

However, efficiency of BTZ is not sufficient against several solid tumors. Therefore, scientists have been designing new systems to enhance BTZ activity as a pH triggered smart biomaterial [90]. For example, Cheng group [90] presented a study by using boronic moieties of BTZ. They designed a dendrimer with catechol groups, the boronic acid moieties on the BTZ were conjugated by boronate ester formation, and these compounds were placed in the interior of the nanostructure at physiological pH. However, *in vivo* and *in vitro* studies showed that BTZ release was accelerated at tumor microenvironment, which has a slightly acidic medium.

Therefore, designed systems improved the biocompatibility, stability, and blood circulation time of drug and decreased non-specific cellular uptake and these

properties make pH triggered drug delivery system a promising candidate for future studies [89-93].

Moreover, Lin et al [64] used boronic acid for selective saccharide sensing. In their study, magnetic iron oxide nanoparticles (Fe_3O_4 MNPs) modified with aminophenylboronic acid were designed to separate glycoproteins from the protein mixtures. Boronic acids on the particles formed complexes with glycoproteins such as cellulose and ovalbumin; however, they did not interact with bovine hemoglobin, bovine serum albumin and lysozyme which are non-glycoproteins. After fast and selective binding to glycoproteins, nanoparticles were taken apart from the solution by magnetic separation with glycoproteins. This system was specifically tested to separate ovalbumin from the egg white sample [64].

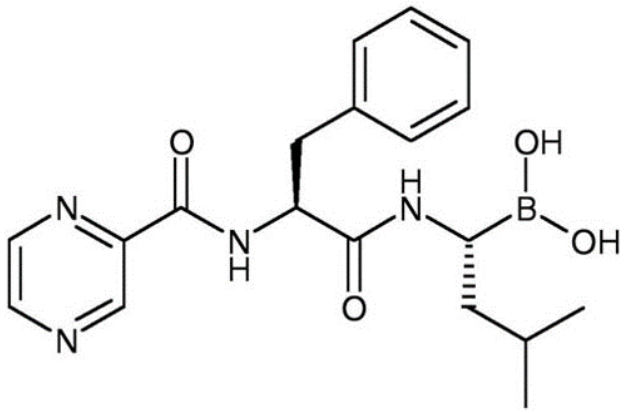

Figure 1.13 The chemical structure of Bortezomid

Moreover, Shen et al utilized boronic acid for blood sugar detection without any enzymatic reaction [94]. Boronic acid modified C-dots based fluorescent sensors were designed to detect the glucose concentration in the blood. Boronic acid based

systems are generally preferred due to easy usage, high efficiency, and selectivity for blood sugar quantification. This chemosensor exhibited selectivity from 9 to 900 μM glucose concentration that exhibited higher sensitivity than the previous fluorescent based studies of boronic acid. Addition of glucose into boronic acid functionalized C-dot systems led to change in fluorescence intensity because diol moieties of glucose bind to boronic acids on the C-dot covalently which resulted in a decrease in distances between C-dots and hence, fluorescence quenching was observed [94].

Chapter 2

Material And Methods

2.1 Introduction

Targeted drug delivery in cancer remains one of the major clinical problems. To solve this problem, scientists have tried to find differences between cancerous and healthy tissues. Cancer environment possesses a slightly acidic pH than the healthy tissue; therefore, stimuli responsive materials have drawn attention for targeted drug delivery applications. Boronic acid is one of the most important stimuli responsive molecules which can form a bond with vicinal diols such as saccharide or catechols reversibly. While the bond formation is triggered in neutral pH, these bonds are weakened under slightly acidic conditions [33, 50, 51].

In this study, boronic acid and DOPA conjugated peptide amphiphiles were designed to obtain a controllable drug release system. The oppositely charged boronic acid/DOPA conjugated peptide amphiphiles were mixed to form nanofibers by molecular self- assembly via noncovalent interactions and these molecules are placed

on the nanofiber surface. Due to charge neutralization, mixing at higher concentrations forms aggregates and hydrogel formation occurs.

Besides these, boronic acid/DOPA molecules formed intramolecular reversible crosslinks which increase the strength and self-healing capability of hydrogels at neutral pH. These hydrogels represent suitable behavior for controlled drug release systems.

Furthermore, boronic acid/DOPA crosslinks demonstrate pH triggered system and at mildly acidic conditions, the interactions weaken (Scheme 2.1). In this study, Doxorubucin-HCl (Dox) was selected as a release molecule which is a well-known cancer drug that is fluorescence and UV-Vis active. Thus, quantitative and qualitative analysis of Dox can be performed by spectroscopic methods [95, 96]. These make Dox a suitable candidate for various drug release systems.

To test the drug encapsulation and pH dependent release profile, Dox was encapsulated inside the hydrogel network and their behavior was observed at pH 7.4 and 5.5. Moreover, DOPA/E_3-PA, boronic/K_3-PA and E_3/K_3-PA groups were also analyzed as a control group to distinguish the exact effect of the boronic acid/DOPA interaction.

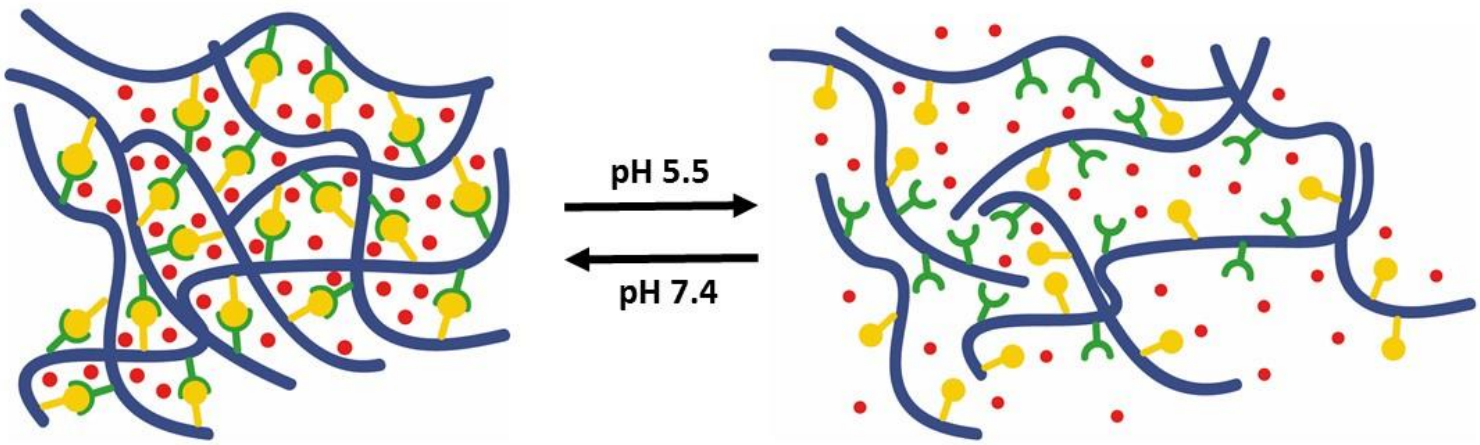

Figure 2.1 Schematic representation of Boronic/DOPA -PA hydrogel network at different pH

2.2 Experimental Section

2.2.1 Chemicals and Reagents

Chemicals and reagents that are used during synthesis of peptide amphiphile molecules, hydrogels preparation, and their analysis can be seen below.

2.2.2 Chemical and Reagents to Synthesis Peptide Amphiphile Molecules

[4-[α-(2',4'-dimethoxyphenyl) Fmoc-aminomethyl] phenoxy] acetamido norleucyl-MBHA resin (Rink amide MBHA resin), 2-(1H-Benzotriazol-1-yl)-1,1,3,3 tetramethyluronium hexafluorophosphate (HBTU), other protected amino acids were purchased from NovaBiochem. 4-carboxylphenylboronic acid, N,N-Diisopropylethylamine (DIAE), dichloromethane (DCM), dimethylformamide (DMF), doxorubicin hydrochloride, piperidine, acetic anhydride, trifluoroacetic acid (TFA) were purchased from Fisher, Merck, Alfa Aesar or Sigma Aldrich. Other chemicals used in characterization such as acetonitrile, 3,4-Dihydroxy-9,10-dioxo-2-anthracenesulfonic acid sodium salt (Alizarin Red S), uranyl acetate, 4-(2-hydroxyethyl)-1-piperazineethanesulfonic acid (HEPES), 2-(N-Morpholino)ethanesulfonic acid, 4-Morpholineethanesulfonic acid (MES) were purchased from Sigma Aldrich and Merck.

2.2.3 Synthesis and Characterization of PAs

By using solid phase peptide synthesis (SSPS) Boronic Acid-EEEGAVVK-(Lauryl)-Am (Boronic-PA), Ac-EEEGAVVK-(Lauryl)-Am (E_3-PA) Lauryl-VVAGKKK-DOPA (DOPA-PA), Lauryl-VVAGKKK (K_3-PA), was synthesized on the solid support, Rink amide MBHA resin. 4-Carboxylphenyl-boronic acid and Fmoc-DOPA

(Acetonide)-OH were used as a precursor of boronic acid and DOPA respectively. For amino acid coupling 2 equivalents of F-moc protected amino acid, 3 equivalent of N,N-diisopropylethylamine (DIEA) and 1.95 equivalents of HBTU in DMF were used. The coupling incubation time was 6 h then to acetylate the unreacted amine groups and block the formation of side sequences 10% acetic anhydride/DMF solution had been added for 30 min before Fmoc protecting groups were cleaved by 20% piperidine/dimethylformamide (DMF) solution for 20 min. Trifluoroacetic acid (TFA): triisoproplysilane (TIS): water mixture was administered for 2.5 h in the ratio of 95:2.5:2.5 to cleave the peptide from solid support and transfer toward liquid phase. After each step, the solid support was washed with DCM and DMF to remove the remaining chemicals. To obtain cleaved peptide from solid support, DCM washing was performed and then rotary evaporatory was used to remove excess TFA and DCM. The remaining viscous peptide solution was precipitated by using diethyl ether at -20 °C overnight. The precipitated white pellets were collected by centrifugation followed by dissolving in water then frozen at -80 °C and lyophilized until all ice particles were removed.

The synthesized peptide amphiphiles were characterized by an Agilent 6530 series reverse phase high performance liquid chromatography (HPLC) equipped with high resolution Quadropole Time of Flight (Q-TOF) mass spectrometer with electron spray ionization source (ESI). One mg/mL K_3-PA and DOPA-PA molecules prepared in double distilled water (dd-water) and as a column Agilent Zorbax Extend-C18, 3.5 µm 80A (100 x 4.6 mm) was used as the mobile phase water (0.1% formic acid)/acetonitrile (0.1% formic acid) gradient was performed. On the other hand, an Agilent Zorbax 300SB-C18, 3.5 µm (100 x 4.6 mm) column and water

(0.1% NH4OH)/acetonitrile (0.1% NH4OH) gradient was used as a mobile phase for E3-PA and Boronic-PA characterization. Absorbance at 220 nm was used for chromatograms.

2.3.4 Preparative High Performance Liquid Chromatography (Prep-HPLC)

To purify the E_3-PA and K_3-PA, Agilent 1200 preparative reverse-phase HPLC system was performed and 10 mg sample was dissolved in 1 ml water (0.1% TFA or NH_4OH). For positively charged peptide, Zorbax prepHT 300CB-C8 column with a water/acetonitrile (0.1% TFA) gradient was used followed by HCl treatment for TFA removal. Furthermore, for negatively charged E_3-PA Gemini 5µ C18 110A column with size of 100 × 21.20 mm and water/acetonitrile (0.1% NH_4OH) gradient was used. DOPA-PA was pure enough for usage; so in order to remove excess TFA, only HCl treatment was performed. Moreover, to remove the excess TFA and impurities, dialysis was performed for 2 days.

2.3.5 Zeta Potential Measurements of PAs

2 mM K_3-PA, E_3-PA, DOPA-PA, boronic-PA and their coassembled combinations were mixed and the solutions were incubated at pH 7-8 at room temperature in order to observe the charge distribution of negatively and positively charged peptide solutions and their coassembled structures. Further, they were diluted to 250 µM with water and measured by Malvern Nano-ZS Zetasizer by using a dip cell electrode in quartz cuvettes. Standard deviations were calculated from the mean of the data of repetitive experiments ($n \geq 3$).

2.3.6 Transmission Electron Microscopy (TEM)

2 mM DOPA-PA/boronic-PA, DOPA-PA/E_3-PA, boronic-PA/K_3-PA and K_3/E_3-PA solutions were prepared in water and pH was adjusted to 7.4 (physiological pH) and incubated for 2 h at room temperature. Then the samples were diluted to 125 μM and 10 μL samples were dropped on the copper TEM grid and incubated for 5 min. Solution was removed from the grid and the grid was stained with uranyl acetate (2% (w/w)) for 2 min. After withdrawal of excess dye and washing with dd-water, grids were left to dry at room temperature for 15 min. The TEM instrument that is used for morphological characterization of coassembly systems was FEI Tecnai G2 F30 worked at 100 keV.

2.3.7 Scanning Electron Microscopy (SEM)

Morphological characterization and structural analysis of peptide amphiphile hydrogels were monitored by FEI Quanta 200 FEG scanning electron microscope (SEM) instrument equipped with an ETD detector. 10 mM 20 μL oppositely charged peptide amphiphiles were mixed on the wafer after 30 min incubation at room temperature and for dehydration steps, the sample was incubated in 20%, 40%, 60%, 80% ethanol for 20 min in each solution and finally in 100% ethanol solutions for 3 h to prevent shrinkage of the gels. Tousimis Autosamdri-815B critical-point-drier (CPD) instrument enables to dry dehydrated form of nanofibers gels without damaging the 3D network. Before SEM imaging, samples were sputter coated with 5 nm of a gold-palladium alloy.

2.3.8 CD Analysis

To analyze the secondary structures of individual PAs and coassembled PA systems

2 mM stock solutions of individual PAs were prepared and sonicated. Then oppositely charged PAs were mixed at 1:1 ratio and incubated at room temperature for 1 h. Next, the samples were diluted to 125 μM at physiological pH and pipetted gently not to damage the self assembled structures. Solutions were placed into 1 mm quartz cuvettes and measured by Jasco J-815 CD Spectrophotometer, whose spectra is between 190 to 300 nm with 0.1 nm data pitch, 4 sec DIT, 1 nm band width, 100 nm/min scanning speed with standard sensitivity. For data analysis, the results were converted as mean residue ellipticity and the unit was transformed to deg.cm^2.dmol.

2.3.9 ARS Based Spectroscopic Measurements

Formation of boronic acid diol bonds cannot be characterized by direct methods for this study. In the literature examples, instead of direct methods, indirect indicator assays are frequently used to determine the boronic acid-diol interactions. ARS dye is one of the most crucial catechol dye used to identify the interaction between diol groups and boronic acid. As the amount of boronic acid-ARS complex increased, fluorescence intensity was also seen to be increased [65.66].

In our study, it was predicted that boronic acid and ARS forms a fluorescence active complex at neutral and mildly acidic solution. At pH 7.4, introduction of DOPA-PA into solution will break the fluorescence active complex and fluorescence intensity of the systems decreases at neutral conditions. However, at pH 5.5, DOPA-PA addition does not affect the fluorescence active complex since DOPA affinity towards boronic acid at this pH is less than its affinity at neutral conditions which is illustrated in scheme 2.2.

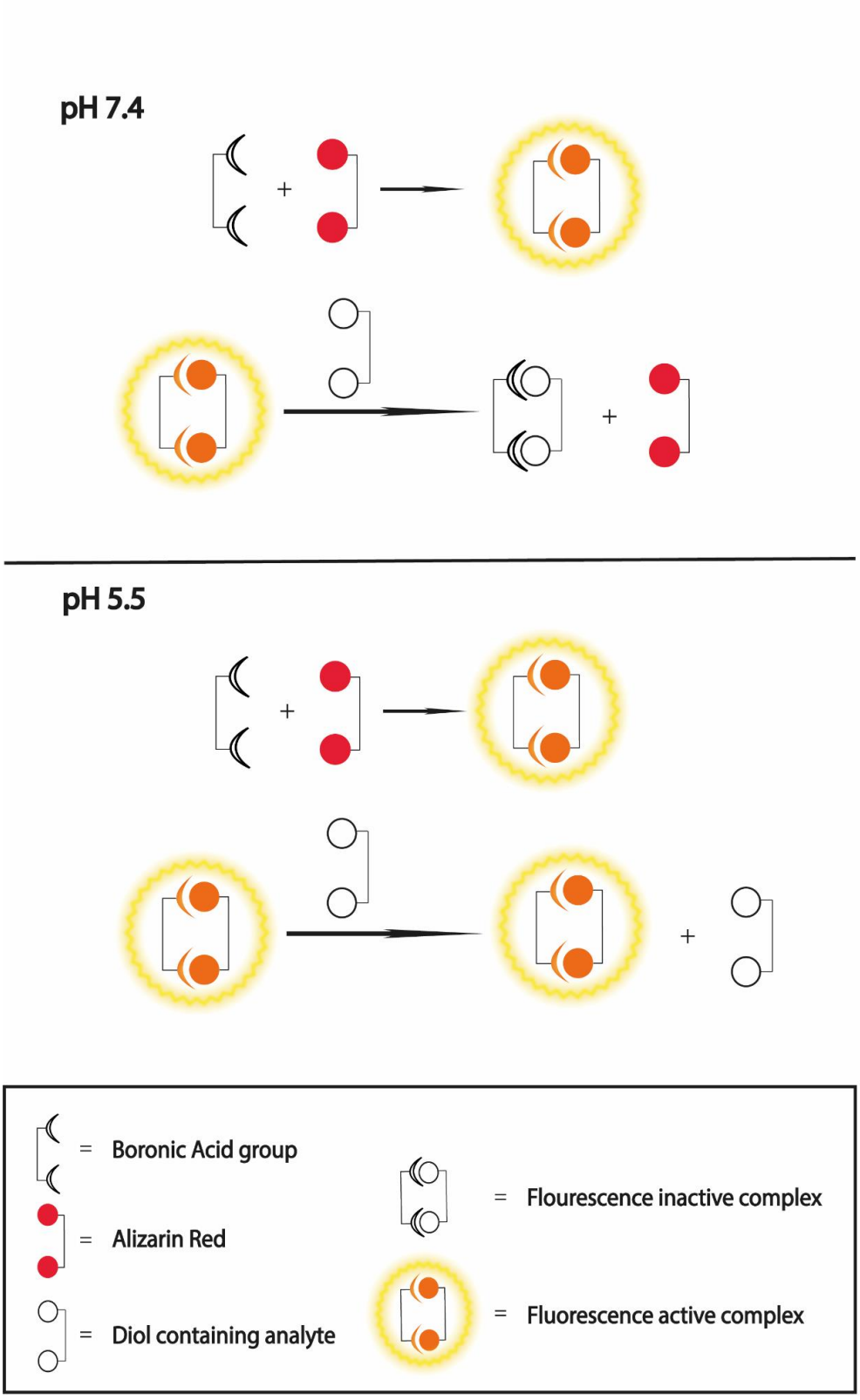

Figure 2.2 Schematic representation of ARS assay

Samples were prepared by mixing 1.5 mM boronic-PA and 100 μM ARS solutions in HEPES or MES buffers and gently pipetting for providing total entanglement. After 30 min incubation, DOPA-PA molecules prepared in different concentration values, were introduced to the solutions and incubated for 1h. To eliminate the side signals and plate emission, solutions without boronic acid were used as a blank solution. Excitation wavelength was chosen as 440 nm and fluorescence intensity was measured by microplate reader.

2.3.10 Rheological Measurements

To investigate the viscoelastic and self-healing (thixotropic) properties of boronic-PA/DOPA-PA, boronic-PA/K_3-PA, DOPA-PA/E_3-PA and E_3/K_3-PA hydrogels, Anton Paar Physica RM301 Rheometer equipped with a 25 mm parallel plate was used. 10 mM positively and negatively charged peptide amphiphiles were mixed in 1:1 ratio to obtain the charge neutralization on the stage. Total volumes of PAs were determined as 300 μL with 500 μm measuring distance from the stage. After achieving gel stability, time dependent rheological analyses were started while strain (0.01%) and angular frequency (10 rad s−1) were kept constant.

By thixotropic analysis, the differences between self-healing properties of boronic/DOPA-PA group and control groups were analyzed. This test composed of 3 phases, load phase was the first step which was applied for the stabilization of gel, second phase was the decomposition phase. In this phase, to weaken the interaction and damage the gel structure, the strain was enhanced logarithmically from 0.01 to 1000% in 1 min. In the third and final phase, that was the recovery phase, gel tried to heal itself at 0.01% shear rate and 10 rad/min angular frequency values.

2.3.11 Release Studies

For cancer drug delivery, the pH differences between the cancerous (slightly acidic pH) and the healthy tissue (neutral pH) were taken into consideration and pH triggered controlled drug release systems were designed. In this study, 10 mM oppositely charged peptide amphiphile and Dox solutions were prepared at physiological pH values. Firstly, positively charged peptide was mixed with Dox solution, vortexed and ultrasonicated to mix the solutions for 5 min. Further, solutions were transferred to cuvettes on the negatively charged peptide solutions by micropipetting in order to form hydrogels via charge neutralization (Figure 2.3). After 12 h incubation at 37 ºC, HEPES buffer (pH 7-7.5) and MES buffer (pH 6-5.5) solutions were gently added onto the gels. As mentioned earlier, Dox molecule is a UV-Vis active molecule and by preparing a standard calibration curve, the amount of the drug released to the buffer was quantified by UV-Vis Spectrophotometer – Cary 100 Bio instrument. Measurements at average time points were taken for 24 h.

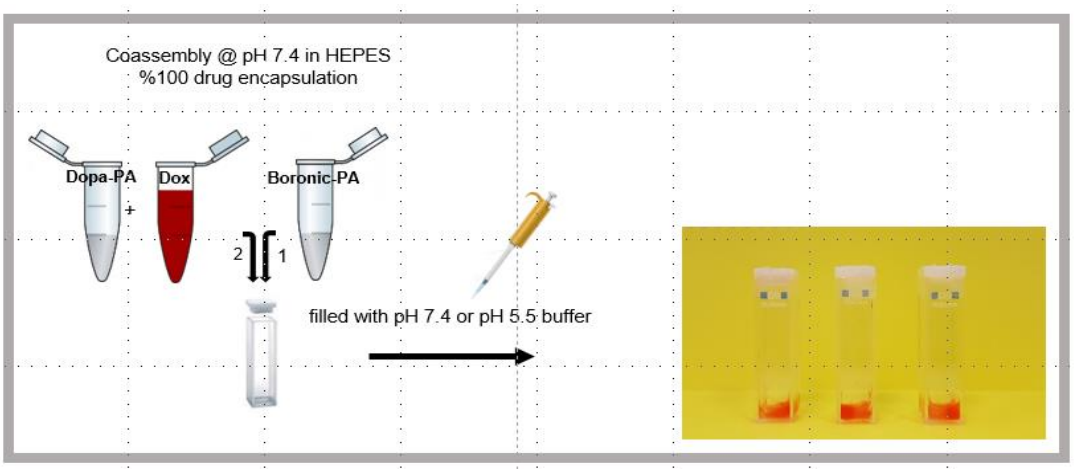

Figure 2.3 Schematic representation of Dox encapsulation inside the PA network.

Chapter 3

Results And Discussion

In this study, peptide amphiphile-conjugated systems were used as an alternative to polymeric systems which are a promising platform due to their biocompatible and biodegradable nature. These PA nanostructures were tailored to exhibit sol-gel transition behaviors in response to external stimuli. This gel like behavior was a result of hydrophobic interaction of carbon tail, electrostatic interactions of oppositely charged residues and hydrogen bonding of backbone [13]. The aim of this study was to form coassembly nanostructures by using oppositely charged boronic acid and DOPA conjugated PA by noncovalent interactions where boronic acid/DOPA units stay on the exterior site of the nanofibers (Figure 3.1). In addition to noncovalent interactions, boronic acid and DOPA moieties present on the peptide nanostructure surface form reversible covalent complexes at physiological pH, which can increase the hydrogel strength, self-healing capacity and entrapment of doxorubicin inside the hydrogel network. However, at acidic pH, these interactions weaken (Figure 2.1) and doxorubicin release accelerates at tumor site.

Negatively charged boronic-PA and positively charged DOPA-PA were used as the main group in this study. Furthermore, E_3-PA and K_3-PA were also used as control groups. Positively and negatively charged PAs were mixed to obtain coassembled nanofiber systems by supramolecular forces at physiological pH and room temperature. DOPA conjugated peptide amphiphiles were selected as cis-diol containing molecules. In fact, there are different cis-diol containing alternatives such as glyco- and catechol containing molecules, which are frequently used for boronic acid studies. However, in this study, DOPA containing system was selected due to several reasons. The most important reason is that boronic acid-PA and DOPA-PA interactions can be detected by indirect characterization methods such as ARS assay. Additionally, a stable hydrogel structure can be designed since DOPA-PA can easily form a crosslinked structure on the built area that increases the adherence capability and surface stability.

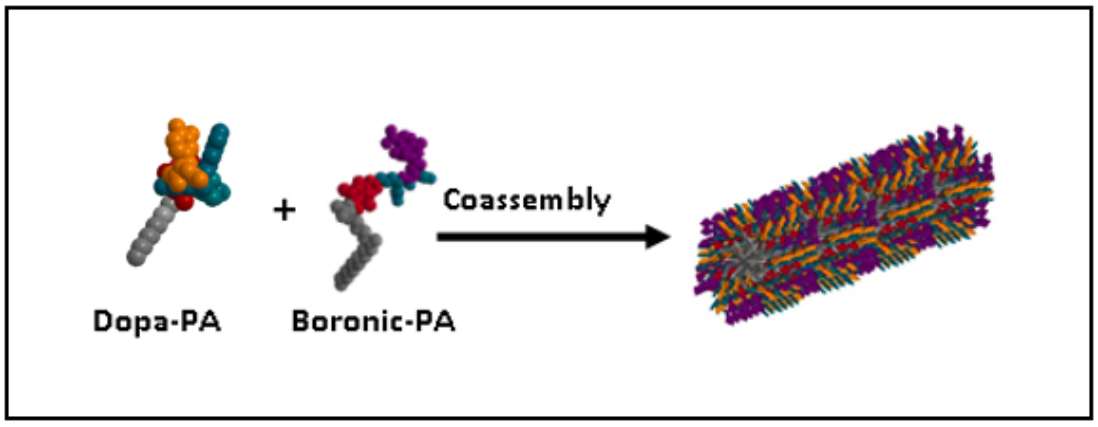

Figure 3.1 Schematic representation of Boronic/DOPA-PA nanofiber formation.

Boronic-PA (Boronic Acid-EEEGAVVK-(Lauryl)-Am) (Figure 3.2a) was synthesized with Fmoc-Lys-(Mtt)-OH as a linker. Firstly, carbon tail was coupled to the Mtt protection site and boronic acid was linked as the last moiety to increase the

coupling efficiency and availability; and as a control, E_3-PA (Ac-EEEGAVVK-(Lauryl)-Am) (Figure 3.4a) was synthesized with the same methods. DOPA-PA (Lauryl-VVAGKKK-DOPA-Am) (Figure 3.3a) and K_3-PA (Lauryl-VVAGKKK-Am) (Figure 3.5a) were also synthesized with direct Fmoc-solid-phase method. After synthesizing all PAs, the molecules were purified or dialyzed to remove the impurities and to obtain a higher purity. The reason of using PAs with three charged residues is that boronic-PA with one glutamic acid had solubility problems under physiological conditions. Moreover, DOPA-PA with single lysine had tendency to form hydrogel itself at high concentrations because this charging is not enough for charge repulsion and they start to self-assemble without requiring the addition of any external molecule for charge neutralization. Boronic-PA/K_3-PA, DOPA-PA/E_3-PA and E_3-PA/K_3-PA combinations were also analyzed for every characterization technique to distinguish the results of individual effects of boronic acid, DOPA and non-conjugated PAs. In our system, PA molecules have an aliphatic tail which triggers the hydrophobic interaction. The -VVAG- amino acid sequence acts as β-sheet forming sequences by hydrogen bonding. Oppositely charged residues –KKK-/-EEE- provide amphiphilicity within the molecule that is responsible for solubility in water. This electrostatic interaction with other noncovalent forces triggered them to form three dimensional nanostructures. The chemical structures of positively and negatively charged PAs were determined by the liquid chromatography equipped with electronspray mass spectrometry (Figure 3.2-5b).

All PA molecules hold three charged amino acids, so 1:1 (v:v) mixing at the same concentration value was required for charge neutralization. In practical to determine the overall charge neutralization, zeta potential measurements of the all PAs

molecules and coassembled PA mixtures were examined (Figure 3.6). As a result, 1:1 (v/v) solutions were determined for approximate neutral coassembly of the systems.

For secondary structure analysis, PA molecules and coassembled PA structures were analyzed by circular dichroism (Figure 3.7). Individual peptide amphiphiles represented a disordered conformation which is also called as random coil structure due to charge repulsion inside the solutions which has a negative peak maxima between 195-200 nm. However, mixing negatively and positively charged PAs triggered the assembly process and molecules formed β-sheet architecture which represented a positive signal at 202 nm and a negative ellipticity approximately at 220 nm. Although boronic-PA/DOPA-PA group represented a strong β-sheet signal at physiologic pH, other groups have weaker signal than the main group. This dichroism intensity change was determined to be named as a β-sheet formation capability in the literature. It was reported that decreasing ellipticity at 218 nm gives information about the β-sheet content of the system. E_3-PA/K_3-PA, boronic-PA/K_3-PA and DOPA-PA/E_3-PA results exhibited feeble signals.

The coassemled PA nanostructures were monitored by TEM imaging. These PAs formed nanofiber structures with a diameter size of approximately 7-10 nm and a length of 30 nm to micrometers (Figure 3.8).

For morphological characterization, three dimensional hydrogel network was visualized by SEM (Figure 3.9). Their original structures were protected by fast exchange between liquid to gas by CPD. These hydrogel structures were utilized as a scaffold and the fiber architecture did not show any difference between the main

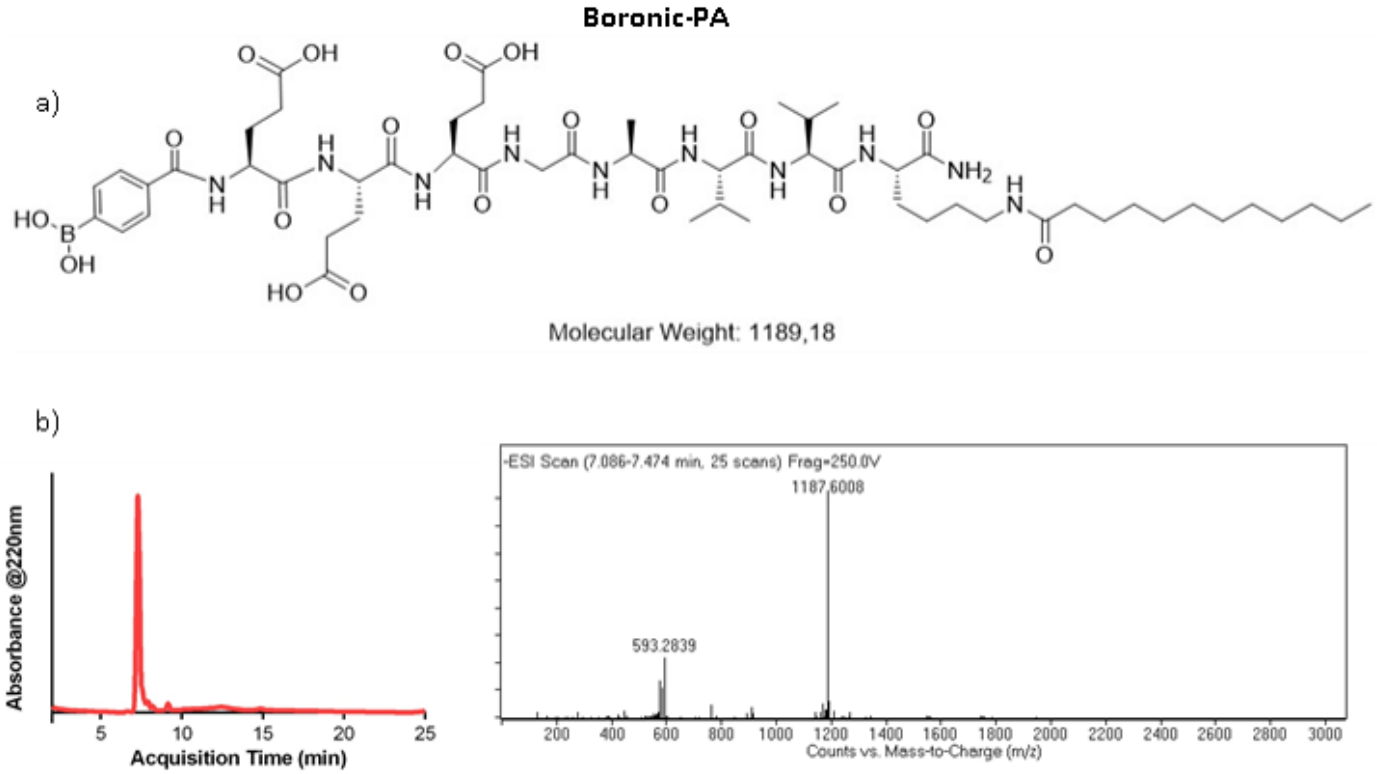

Figure 3.2 a) Chemical structure and b) liquid chromatograms and mass spectra of Boronic acid-PA.

$[M-H]^-$ (calculated) = 1188.18, $[M-H]^-$ (observed) = 1187.6008, (observed $[M-2H]^{2-}$ m/z = 593.2839)

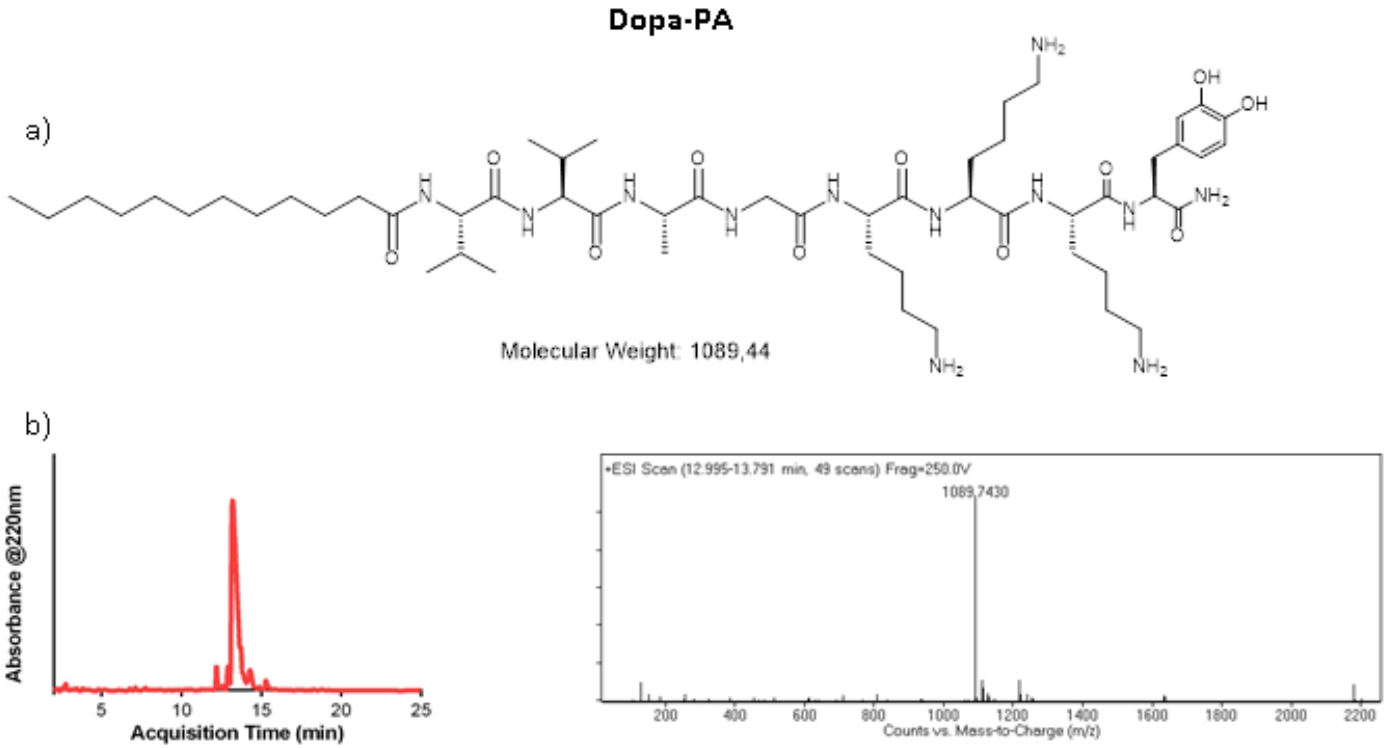

Figure 3.3 a) Chemical structure and b) liquid chromatograms and mass spectra of DOPA-PA.

$[M+H]^+$ (calculated) =1090.44, $[M+H]^+$ (observed) = 1089.7430

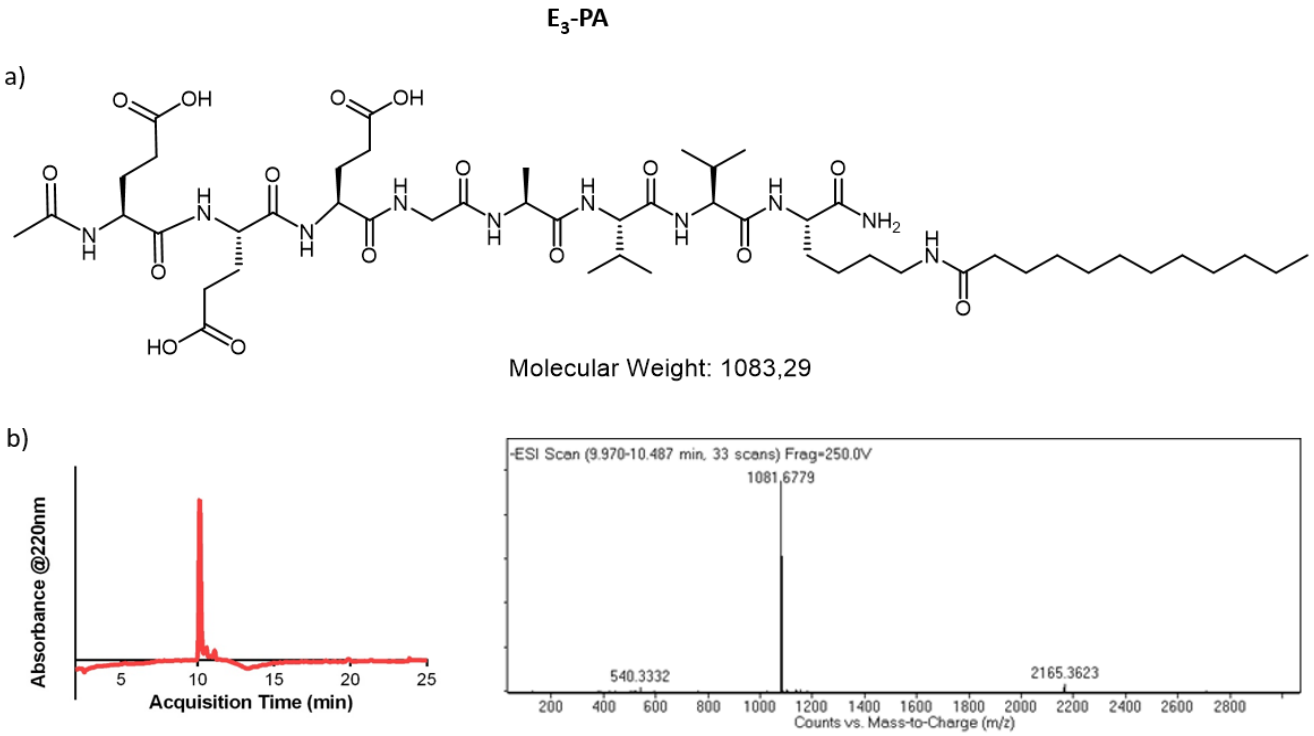

Figure 3.4 a) Chemical structure and b) liquid chromatograms and mass spectra of E_3-PA.

$[M-H]^-$ (calculated) = 1082.29, $[M-H]^-$ (observed) = 1081.6779 (observed $[M-2H]^{2-}$ m/z = 540.3332),

(observed) $[2M-H]^-$ = 2165.3623

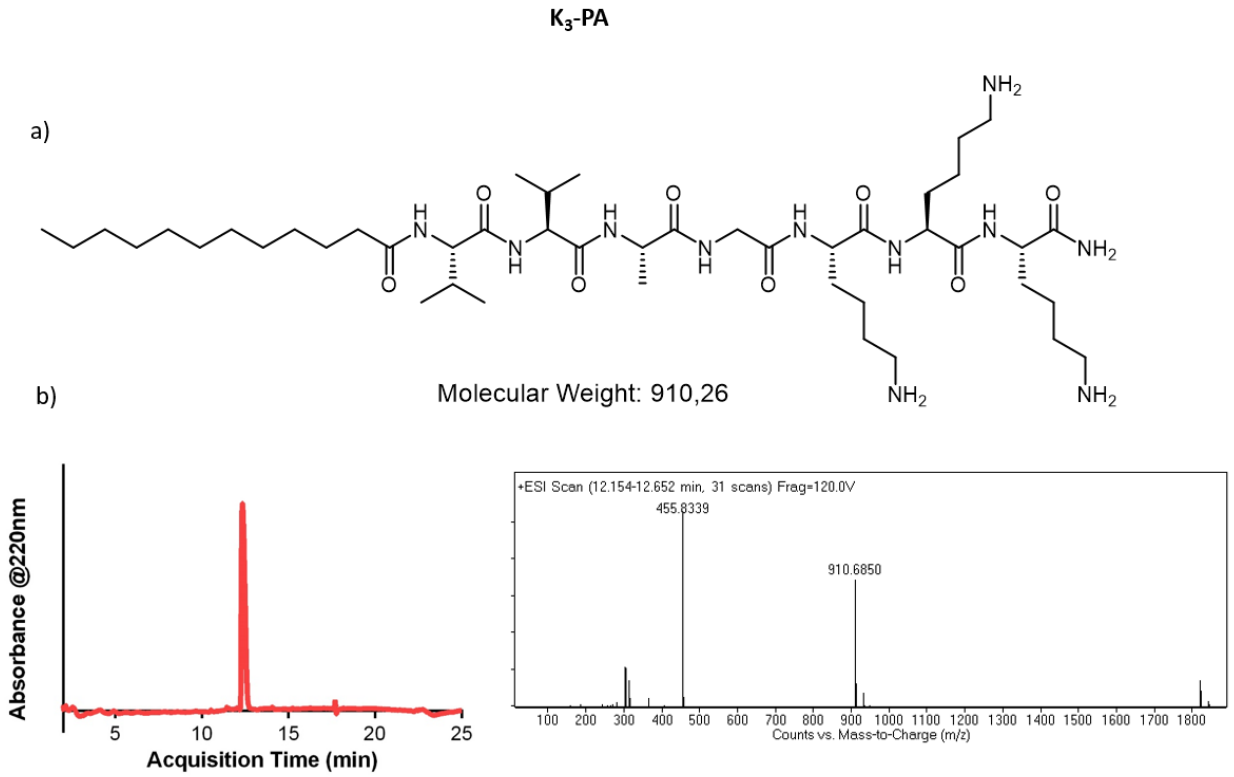

Figure 3.5 a) Chemical structure b) liquid chromatograms and mass spectra of K_3-PA.

$[M+H]^+$ (calculated) =911.26, ($[M+H]^+$ (observed) = 910.6850), $[M+2H]^+$ *m/z* (observed) = 455.8339

	Theoretical Charge	Measured Charge
Boronic / Dopa-PA (1:1)	0	-0.0379
Boronic / K_3-PA (1:1)	0	0.000690
Dopa / E_3-PA (1:1)	0	-0.0292
E_3 / K_3-PA (1:1)	0	0.0580

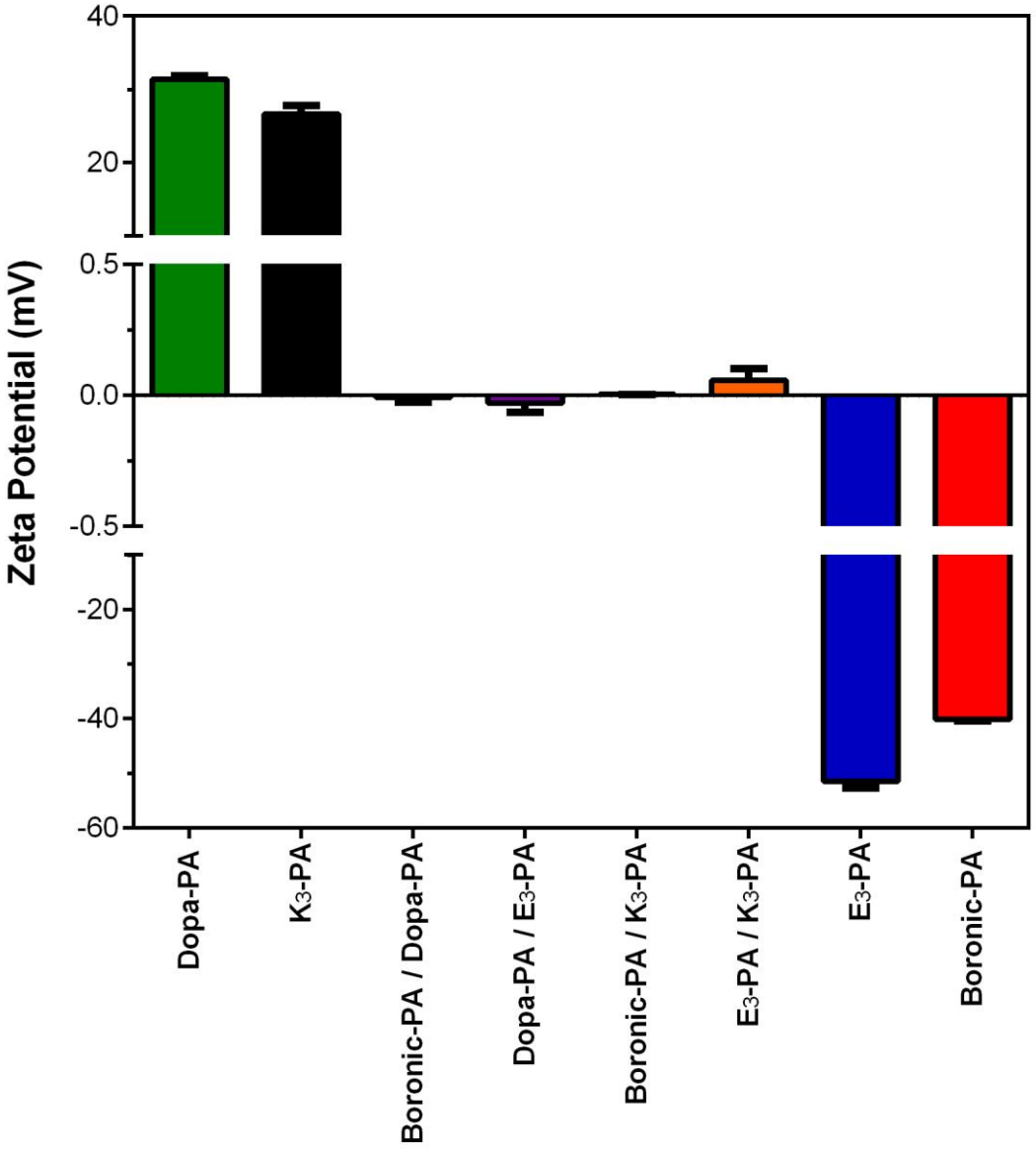

Figure 3.6 The zeta potential results of individual PAs and their coassembled mixtures.

groups and control groups. Following the nanoarchitecture analysis, further chemical analyses were performed.

To determine the reversible covalent complex formation between boronic acid and DOPA molecule, ARS assay was used. As it was explained, it is an indirect method to clarify that there is an interaction between boronic acid and DOPA molecule at specific pH range. Firstly, ARS and boronic-PA were mixed, and then DOPA-PA was introduced to the system.

As it is shown in Figure 3.10a increasing DOPA-PA concentration leads to decrease in fluorescence intensity of the solution, which means that there is an interaction between boronic acid and DOPA molecule that locates on the surface of the coassembled PA structure at physiological pH (pH 7.4).

This is an expected result; however, we also would like to clarify that this interaction was maintained under neutral conditions and at slightly acidic environment; this bond formation is expected to be disrupted in order to build a pH responsive system. So this experimental setup was repeated in pH 5.5 medium.

Figure 3.10b shows that at pH 5.5, addition of different concentrations of DOPA-PA did not result in significant change in fluorescence intensity and all groups have the similar intensities which is a different trend than buffer at physiological pH. As a result, boronate formation was not detected as expected at pH 5.5 for boronic-PA and DOPA-PA system. Boronic-PA/K_3-PA was selected as a control group to understand the selective crosslink between boronic acid/diol groups. At pH 5.5, addition of K_3-PA led to get regular trend; however, the signal changes were not as sharp as

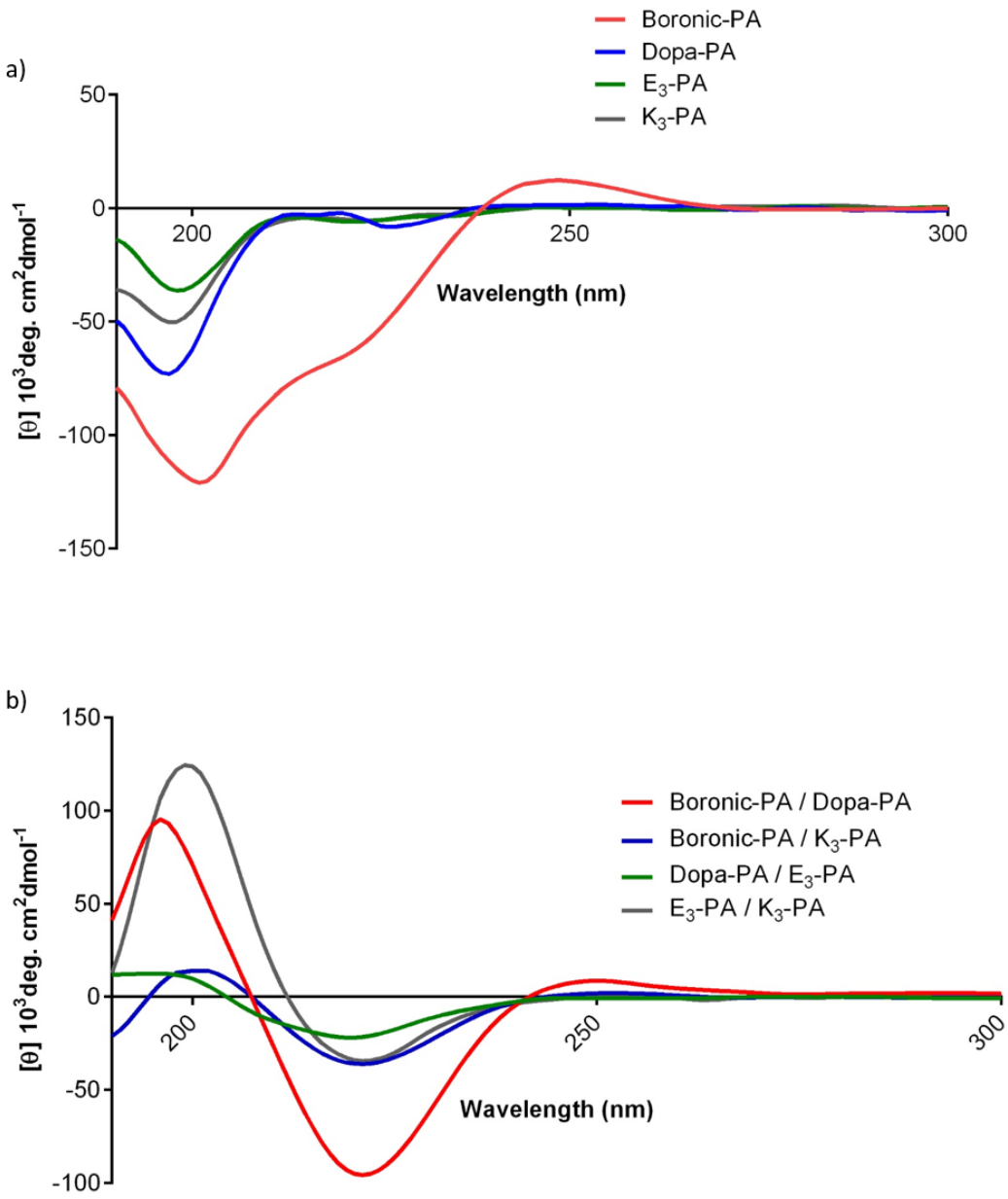

Figure 3.7 The secondary structure analysis of a) individual PA and b) PA mixtures by circular dichroism.

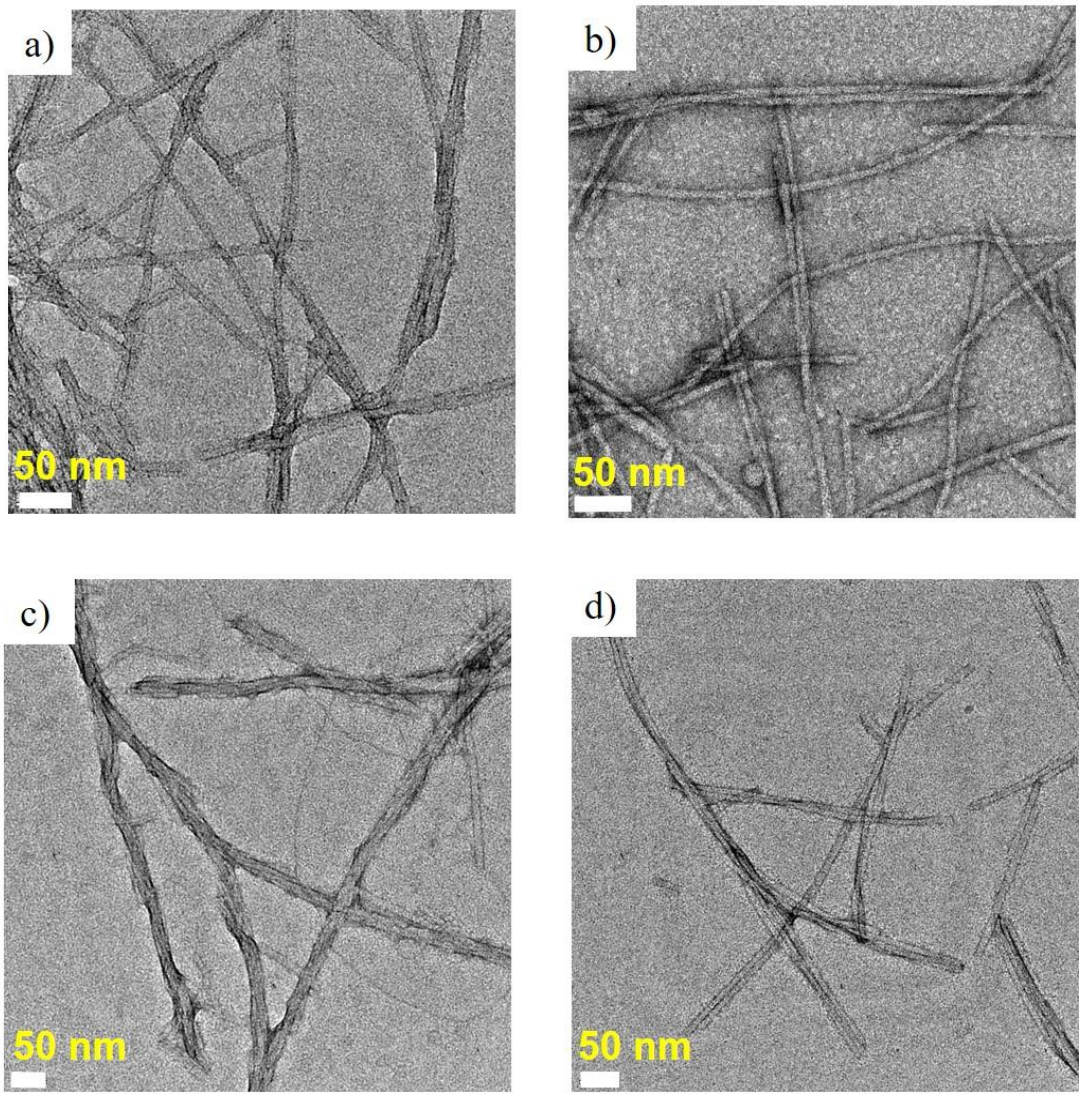

Figure 3.8 TEM images of the a) Boronic/DOPA-PA b) Boronic/K_3-PA c) DOPA/E_3-PA and d) E_3/K_3-PA nanofibers

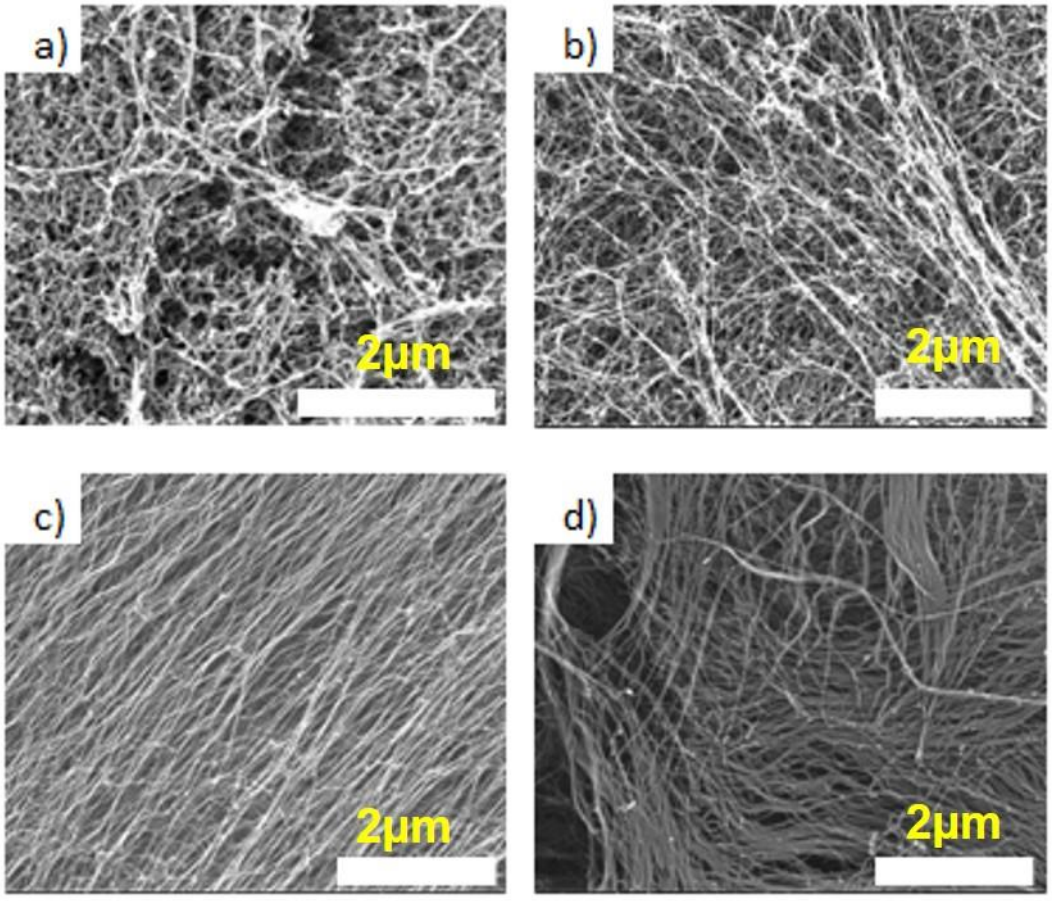

Figure 3.9 SEM images of a) Boronic/DOPA-PA b) Boronic/K_3-PA c) DOPA/E_3-PA and d) E_3/K_3-PA netwoks.

addition of DOPA-PA (Figure 3.10d). This phenomenon could be resulted from the side reaction between oppositely charged PA building blocks at pH 5.5.

On the other hand, at pH 7.4 boronic acid and ARS formed a fluorescent compound. Then, addition of K_3-PA in different concentration did not cause to obtain regular trend and results were different from the addition of DOPA-PA at pH 7.4 (Figure 3.10c). Since K_3-PA is used as a control of non-cis diol containing compounds, so it does not contain any groups which directly interrupt the boronic/ARS compound.

Boronic-Acid/ARS interaction was specified with E_3-PA/DOPA-PA control group at pH 7.4 and 5.5 which is demonstrated in Fig 3.11c,d respectively. Both of these conditions did not show any differences and ARS cannot form fluorescence active compounds. Conclusively, fluorescence intensity that was observed in main group resulted from boronic acid ARS complex.

E_3/K_3-PA group was also utilized in order to investigate the effect of non-conjugated fiber forming sequence on florescence intensity. This group did not give any detectable signal during fluorescent spectroscopy measurements (Figure 3.11a,b).

For measuring the mechanical properties of the hydrogels, hydrogels were prepared only at neutral pH, since slightly acidic conditions were not enough to dissolve the negatively charged PAs. In this study, to equalize the amount of conjugated and controlled PAs, concentrations were determined as 10 mM for all the samples. Dynamic Oscillatory Rheology was performed to investigate the viscoelastic behavior of 4 different combination of PAs. Firstly, time sweep analysis revealed that all groups represented gel-like characteristics which are determined by a higher

storage modulus (G') values than its loss modulus (G") value (Figure 3.12). Same concentrations of coassembled peptide hydrogels were prepared in the same manner.

However, bare E_3/K_3-PA exhibited the lowest storage modulus value among all the groups, where gel structures were modulated via noncovalent interactions between the PA building blocks. Conjugated PA combination showed higher gel strength; since, they can form covalent crosslinks besides noncovalent interactions which can lead to an increase in gel strength. DOPA/DOPA, boronic acid/boronic acid and DOPA/boronic acid intra/inter fiber interactions affected the gel behaviour of conjugated PA groups.

Furthermore, self-healing ability of PAs was examined by thixotropic test technique (Figure 3.13). This technique enables us to clarify the dynamic bond formation effect on gel recovery. High sheer load leads to a decrease in storage modulus until it had a lower value than the loss modulus, which means that the liquid transition from gel like form has occurred. For the recovery step, hydrogen bonds, hydrophobic interactions and electrostatic forces played a role for limited self-healing for E_3/K_3-PA mixtures. Boronic/K_3-PA, DOPA/K_3-PA and boronic/E_3-PA combinations demonstrated higher recovery rate, which can arise from the covalent bond formation after gel damage or protection of covalent bonds during high sheer loading stage.

Finally, our experimental group where the building blocks were boronic-PA and DOPA-PA, exhibited approximately 65-90% recovery ability and this rate could be

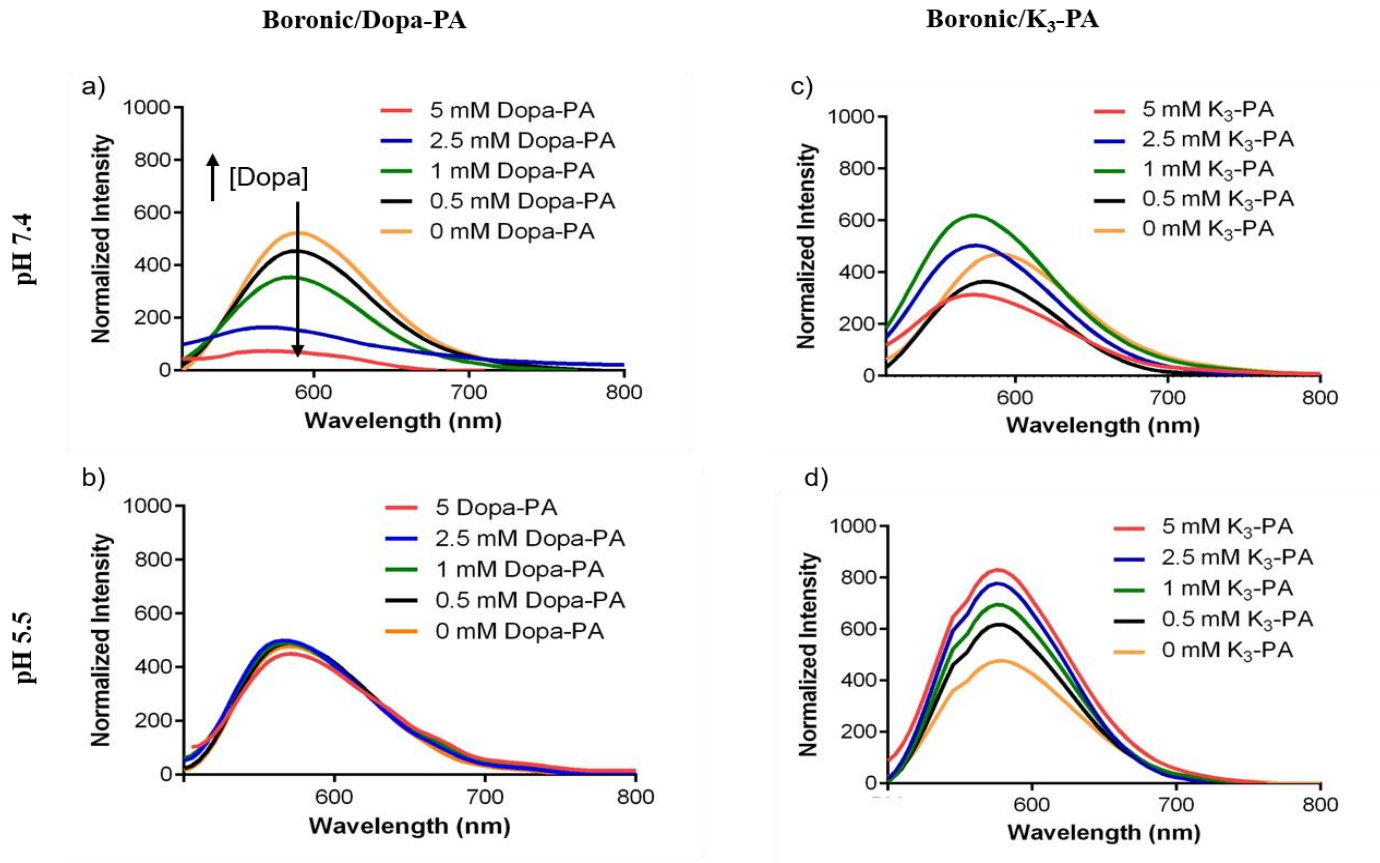

Figure 3.10 ARS assay of a) Boronic/DOPA-PA at pH 7.4 b) Boronic/DOPA-PA at pH 5.5 c) Boronic/K_3-PA at pH 7.4 and d) Boronic/K_3-PA at pH 5.5. ARS: 100µM and Boronic-PA: 1.5 mM. Excitation wavelength: 440 nm

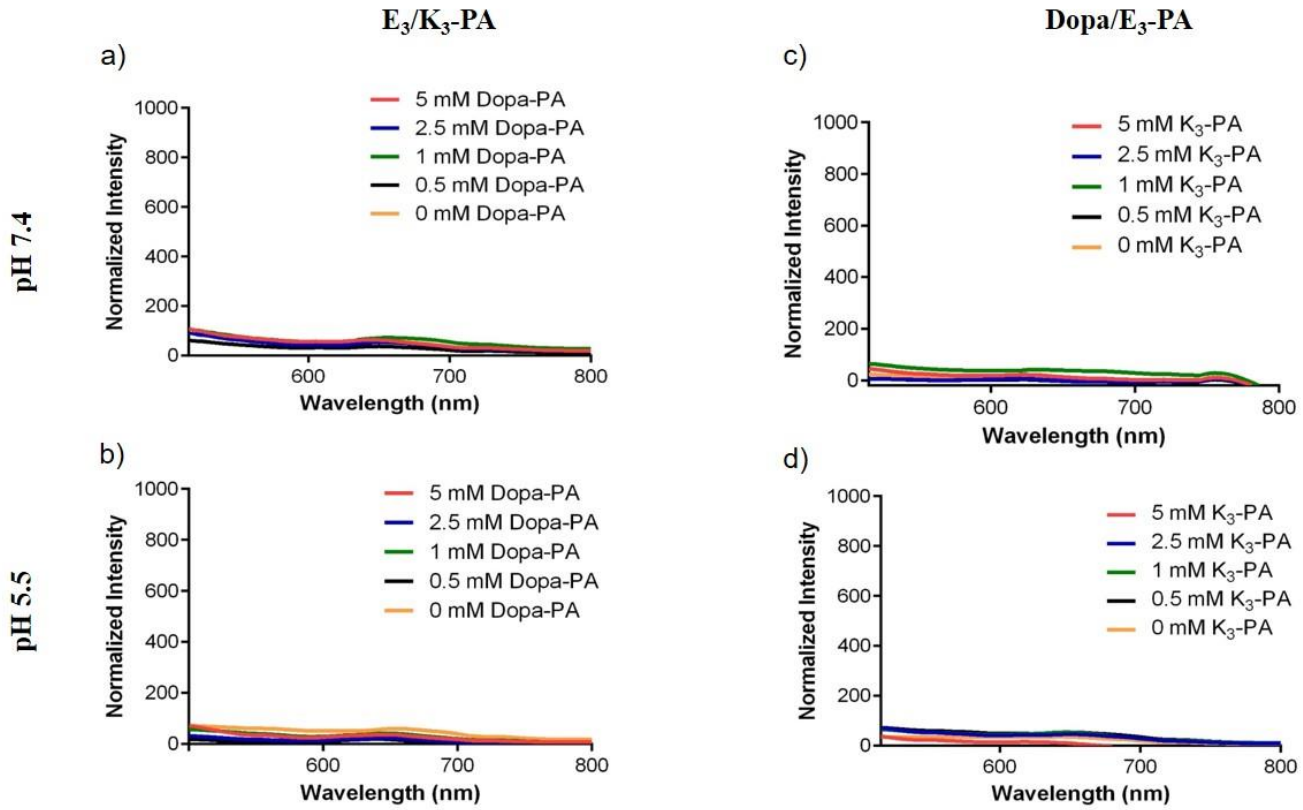

Figure 3.11 ARS assay of a) E_3/DOPA-PA at pH 7.4 b) E_3/DOPA-PA at pH 5.5 c) E_3/K_3-PA at pH 7.4 and d)) E_3/K_3-PA at pH 5.5.

ARS: 100µM and E_3-PA: 1.5 mM. Excitation wavelength: 440 nm

resulted from the reversible covalent crosslink formation. This hydrogel system can be used for further applications but it should be noted that PA hydrogels demonstrate a weaker nature than the polymeric hydrogels because of their limited molecular weight, noncovalent and limited covalent interactions.

For encapsulation procedure, Dox molecule encapsulation was achieved by supramolecular coassembly of the nanofiber network. Homogeneous and 100% encapsulation process was performed at physiological pH.

Supramolecular hydrogel structures have the nanoporous architecture which enables the prevention of burst release and achieves sustained release of Dox molecules that are able to move out the pores. To obtain a pH dependent system boronic acid/DOPA crosslink was used and release experiments were performed at pH 7.4 and 5.5.

In order to identify drug release profiles at different pH values, calibration curve was drawn via measured absorbance values of several concentrations inside the desirable range. After Dox encapsulated gel had been reached the equilibrium, cuvettes were filled with HEPES buffer (pH 7.4) or MES buffer (pH 5.5). Dox diffusion was determined by measuring the absorbance of the samples via UV-VIS Spectrophotometer at average time points (Figure 3.14). These systems were suitable for analyzing the effect of supramolecular self-assembly via only noncovalent interactions (E_3/K_3-PA), supported with covalent interactions (boronic/K_3-PA, DOPA-PA/E_3-PA) or reversible covalent interactions (boronic-PA/DOPA-PA). Therefore, each gel system represented controlled release at pH 7.4 (Figure 3.14a).

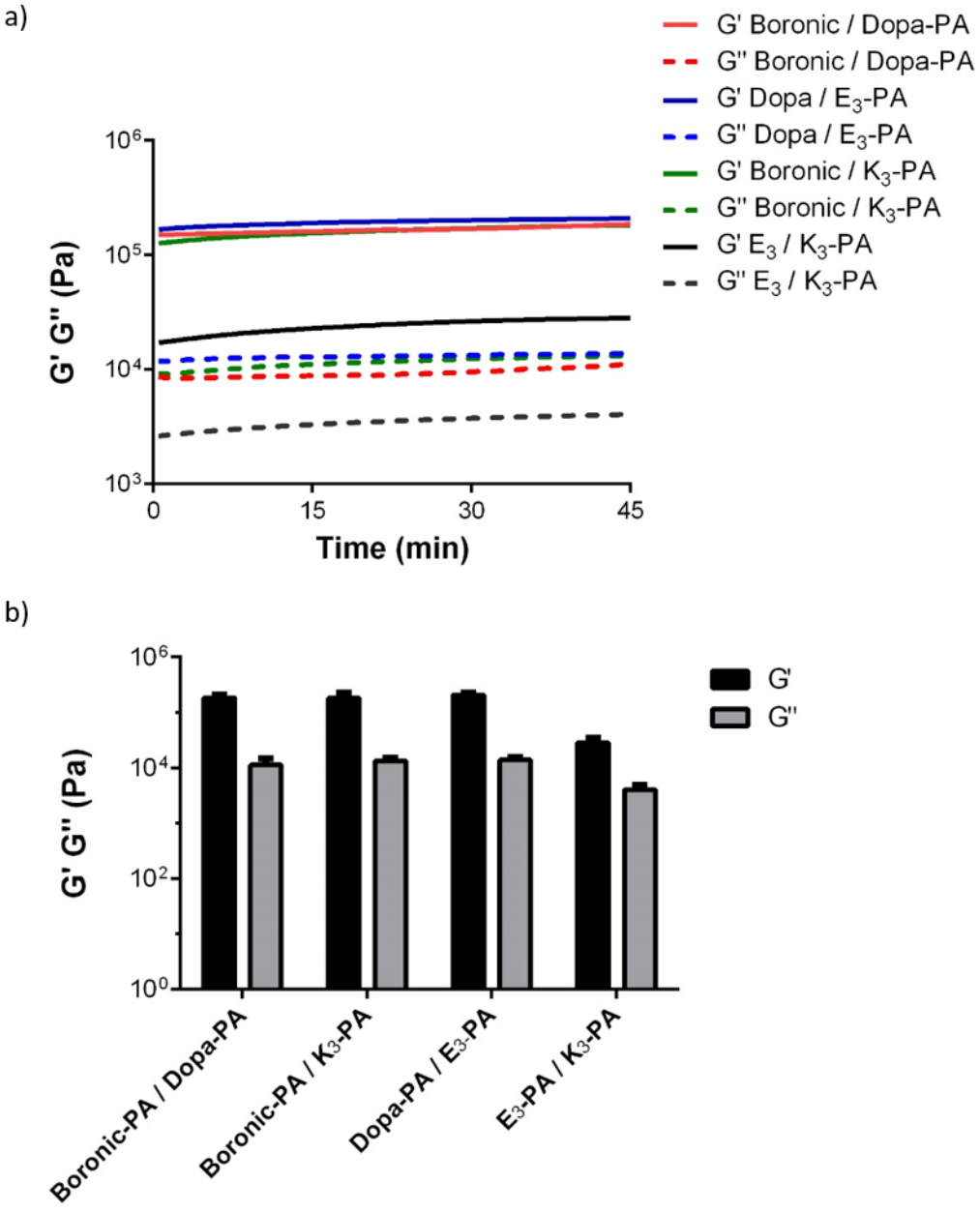

Figure 3.12 Time sweep test of PA mixtures.

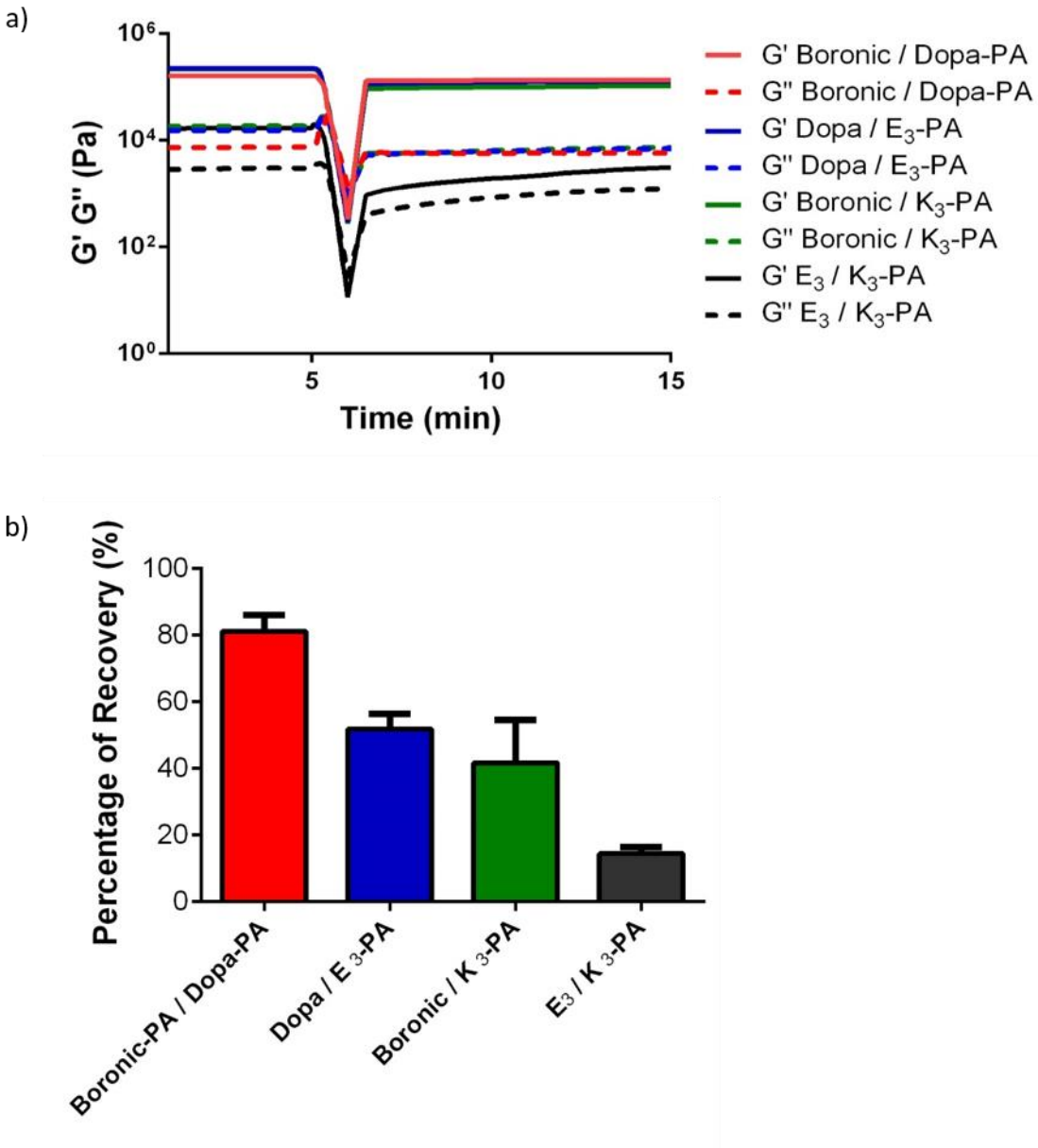

Figure 3.13 a) Thixotropic behavior b) recovery rate of PAs nanofiber gels

Among these groups, boronic-PA/DOPA-PA mixture exhibited less drug release which was approximately up to 10%, which then reached equilibrium at 10 h and burst release was not observed. Then the gels were kept under observation for 24 h and they were observed to protect their stability. These release profiles can result from the intra-fiber covalent crosslinks since these bonds can lead to decrease porous size and Dox cannot escape from the hydrogels. Moreover, the cis-diol groups on Dox leads to binding of boronic acid bearing building blocks at stated conditions, which results in entrapment of the drug inside the gel. At pH value 5.5, boronic/DOPA-PA group demonstrated a higher release rate than pH 7.4 and it reached the equilibrium with around 40% (Figure 3.14b).

Similarly, Dox release from E_3/K_3-PA in MES buffer was higher than HEPES buffer (Figure 3.15). Boronic/K_3-PA exhibited highest variation at different media and even it seemed like a suitable system for cancer treatment, its stability at pH 7.4 was not as desired as the main group and at pH 5.5, other groups did not give consistent results along with a gel degradation. DOPA-PA/E_3-PA did not demonstrate significant difference between the two different pH values after 24h (Figure 3.15). As a result, due to high encapsulation efficiency at pH 7.4 and controlled drug release profile at pH 5.5, boronic/DOPA-PA hydrogel system represents the most promising system for the cancer therapy.

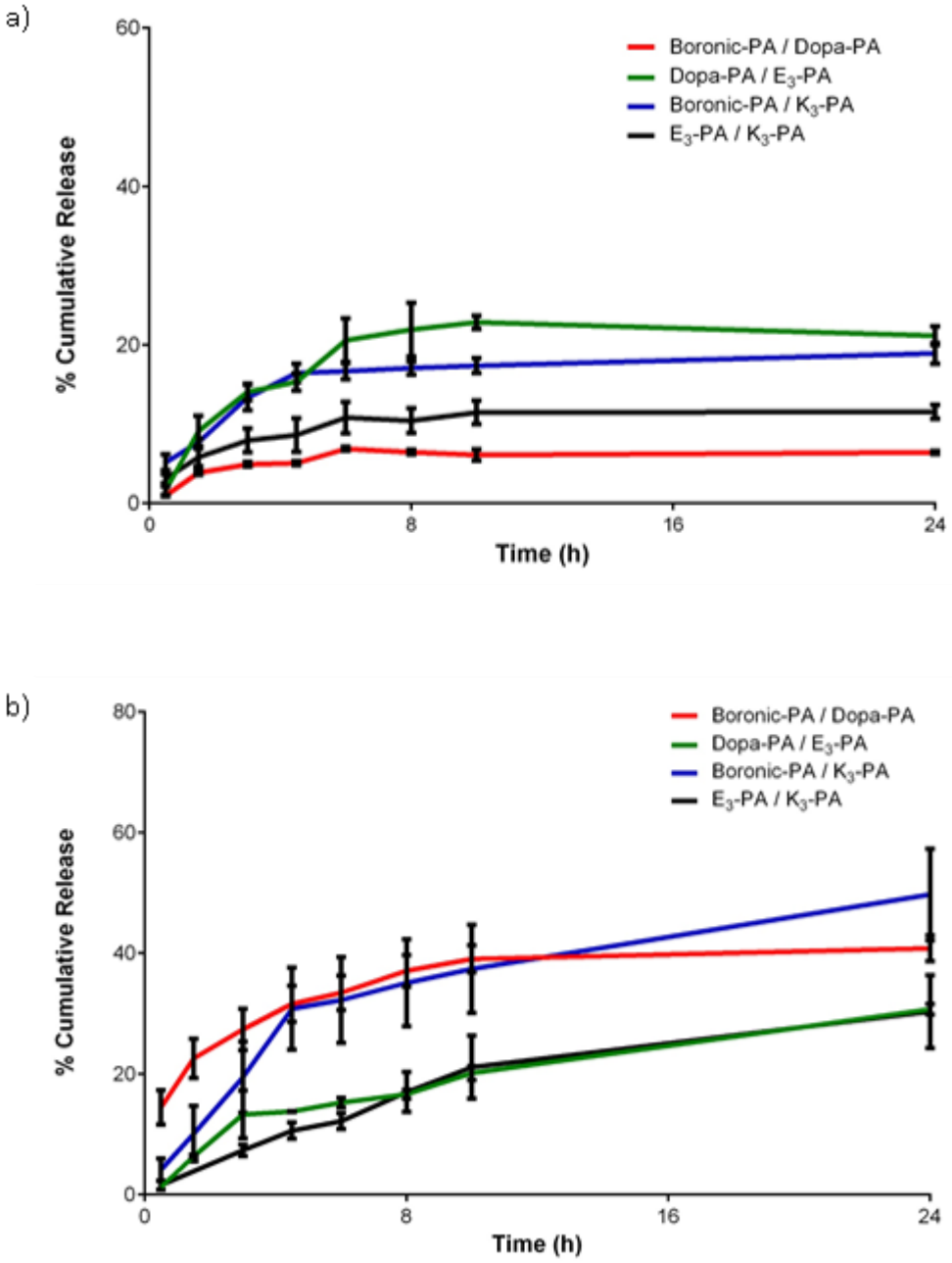

Figure 3.14 Rate of cumulative release profile of Dox through the PA gels at pH 7.4 in HEPES buffer b) pH 5.5 in MES buffer

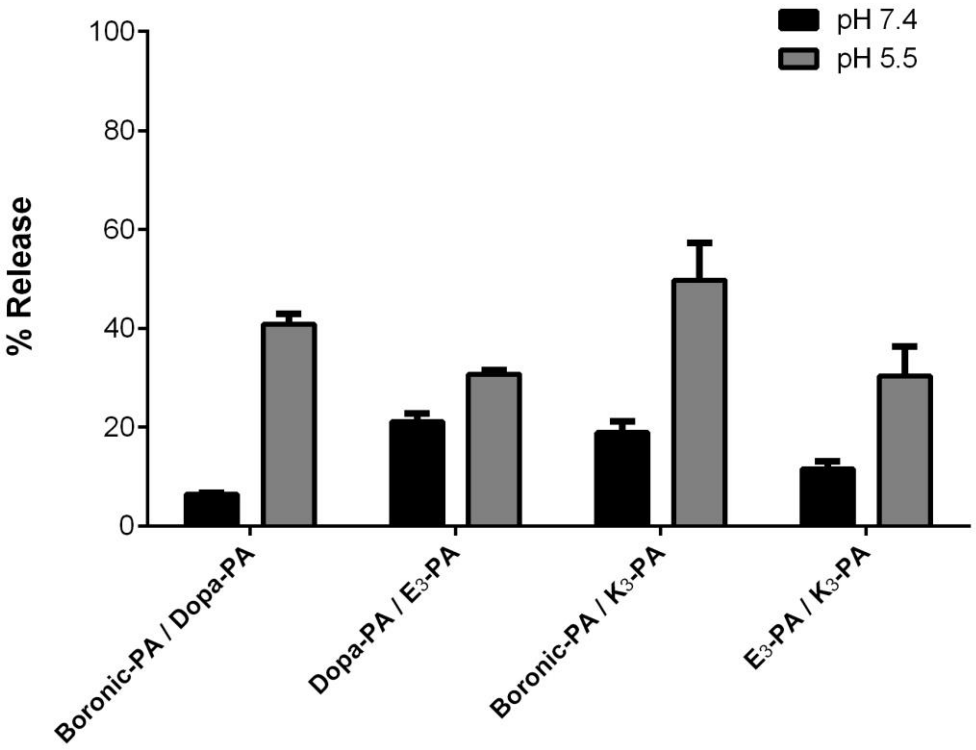

Figure 3.15 Relative release of Dox through the PA gels after 24h

Chapter 4

Conclusion

Self-assembly plays a crucial role in nature to form complex and sophisticated structures. Scientists are inspired from natural self-assembled nanostructures that are self modulated depending on environmental conditions via noncovalent interactions [1, 7]. Peptide amphiphiles are promising building blocks to build supramolecular nanostructures with various properties for several applications such as diagnosis, sensing or targeted drug delivery [24, 36, 97].

In this thesis, by conjugation of peptide amphiphile with boronic acid or DOPA, coassembled systems are formed in order to design controlled drug release systems. These molecules can form reversible covalent bonds, which enable controlled drug release in a pH dependent manner.

Boronic acid and DOPA conjugated peptide amphiphiles and their control groups, E_3-PA and K_3-PA, were synthesized by SPPS method. Firstly, peptide amphiphile molecules were characterized by LC-MS followed by a purification by Prep-HPLC

or dialysis to obtain more than 90% purity. The oppositely charged PA mixtures in 1:1 ratio lead to formation of neutral systems as confirmed by Zeta Potential measurement. These coassembled systems demonstrated a β-sheet secondary structure characterized by CD Spectrometer at physiological pH. Morphological analyses were conducted by SEM and TEM. For TEM, 125 μM PA solutions were prepared and stained with uranyl acetate on the copper grid. For all combinations, TEM images showed that nanofibers with similar length and diameter were formed. Then 10 mM individual peptides were combined to observe the hydrogel network by SEM. Similarly, all mixtures fabricated 3D network with nanofibers.

To understand the interaction between boronic acid and DOPA moieties, indirect indicator assay was applied at two different pH values; pH 5.5 and 7.4. The changed in fluorescence intensity gave information about the interaction between boronic acid and DOPA. As a result, it can be concluded that boronic acid and DOPA molecules formed crosslinks at physiological pH; however, at mildly acidic pH, this crosslinked structures was not observed. It was assumed that boronic acid and DOPA moieties on the nanofiber surface can form pH triggered intramolecular crosslinked structure which lead to increase hydrogel strength and the self-healing properties because boronic acid can form reversible bonds with DOPA. To test the gel strength and recovery rate, rheometric analyses were conducted at pH 7.4. Time sweep measurements showed that boronic acid or DOPA containing coassembled systems showed high mechanical strength than the nonconjugated E_3/K_3-PA groups. Moreover, thixotropic analysis demonstrated that boronic/DOPA-PA mixture showed high recovery rate due to the reversible covalent bond formation.

Release studies were performed in two different buffers; HEPES (pH 7.4) and MES (pH 5.5) to analyze the pH effect on Dox release from the hydrogels at physiological temperature 37 ºC. The Dox amount inside the solution was measured by UV-VIS Spectroscopy and calculated by the calibration curve. Among all hydrogel groups, more stable Dox encapsulation was demonstrated by the boronic/DOPA hydrogel during 24h. No burst release was observed and approximately 9% of encapsulated Dox released after 24h. However, at pH 5.5, Dox release was accelerated and 40% of Dox was observed to be released to the solution. Release amount was 5 time higher at pH 5.5 but still, there was a controlled release which is needed to keep the dosage at therapeutic levels. As a result, boronic acid/DOPA-PA system demonstrated desired behavior as a controlled drug release system.

As a conclusion, in this study, we achieved an increase in peptide amphiphile gel strength, self-recovery ability and pH responsive release by conjugation. The designed system is suitable for further *in vitro* and *in vivo* studies and by designing the sequence of peptide amphiphile molecules, new stimuli responsive peptide amphiphile systems can be prepared.

Bibliography

[1] S. Zhang, "Fabrication of novel biomaterials through molecular self-assembly," *Nature biotechnology,* vol. 21, no. 10, p. 1171, 2003.

[2] G. M. Whitesides and B. Grzybowski, "Self-assembly at all scales," *Science,* vol. 295, no. 5564, pp. 2418-2421, 2002.

[3] G. A. Ozin *et al.*, "Nanofabrication by self-assembly," *Materials Today,* vol. 12, no. 5, pp. 12-23, 2009.

[4] A. C. Mendes, E. T. Baran, R. L. Reis, and H. S. Azevedo, "Self-assembly in nature: using the principles of nature to create complex nanobiomaterials," *Wiley Interdisciplinary Reviews: Nanomedicine and Nanobiotechnology,* vol. 5, no. 6, pp. 582-612, 2013.

[5] P. A. Monnard and D. W. Deamer, "Membrane self-assembly processes: Steps toward the first cellular life," *The Anatomical Record,* vol. 268, no. 3, pp. 196-207, 2002.

[6] J. A. Elemans, A. E. Rowan, and R. J. Nolte, "Mastering molecular matter. Supramolecular architectures by hierarchical self-assembly," *Journal of Materials Chemistry,* vol. 13, no. 11, pp. 2661-2670, 2003.

[7] J. D. Hartgerink, E. Beniash, and S. I. Stupp, "Supramolecular chemistry and self-assembly special feature: peptide-amphiphile nanofibers: a versatile scaffold for the preparation of self-assembling materials," *Proceedings of the National Academy of Sciences of the United States of America,* vol. 99, no. 8, p. 5133, 2002.

[8] M. S. Ekiz, et al., "Self-assembled peptide nanostructures for functional materials," *Nanotechnology,* vol. 27, no. 40, p. 402002, 2016.

[9] H. Lodish, A. Berk, S. L. Zipursky, P. Matsudaira, D. Baltimore, and J. Darnell, "Hierarchical structure of proteins," 2000.

[10] R. Fairman and K. S. Åkerfeldt, "Peptides as novel smart materials," *Current opinion in structural biology,* vol. 15, no. 4, pp. 453-463, 2005.

[11] D. M Leite, E. Barbu, G. J Pilkington, and A. Lalatsa, "Peptide self-assemblies for drug delivery," *Current topics in medicinal chemistry,* vol. 15, no. 22, pp. 2277-2289, 2015.

[12] S. Toksoz, H. Acar, and M.O. Guler, "Self-assembled one-dimensional soft nanostructures," *Soft Matter,* vol. 6, no. 23, pp. 5839-5849, 2010.

[13] S. Toksöz, and M. O Guler, "Self-assembled peptidic nanostructures," *Nano Today,* vol. 4, no. 6, pp. 458-469, 2009.

[14] Y. Chen, H. X. Gan, and Y. W. Tong, "pH-controlled hierarchical self-assembly of peptide amphiphile," *Macromolecules,* vol. 48, no. 8, pp. 2647-2653, 2015.

[15] T. J. Moyer, J. A. Finbloom, F. Chen, D. J. Toft, V. L. Cryns, and S. I. Stupp, "pH and amphiphilic structure direct supramolecular behavior in biofunctional assemblies," *Journal of the American Chemical Society,* vol. 136, no. 42, pp. 14746-14752, 2014.

[16] J. D. Hartgerink, E. Beniash, and S. I. Stupp, "Peptide-amphiphile nanofibers: a versatile scaffold for the preparation of self-assembling materials," *Proceedings of the National Academy of Sciences,* vol. 99, no. 8, pp. 5133-5138, 2002.

[17] M. J. Pandya, E. Cerasoli, A. Joseph, R. G. Stoneman, E. Waite, and D. N. Woolfson, "Sequence and structural duality: designing peptides to adopt two stable conformations," *Journal of the American Chemical Society,* vol. 126, no. 51, pp. 17016-17024, 2004.

[18] S. Fleming and R. V. Ulijn, "Design of nanostructures based on aromatic peptide amphiphiles," *Chemical Society Reviews,* vol. 43, no. 23, pp. 8150-8177, 2014.
[19] A. Aemissegger, V. Kräutler, W. F. van Gunsteren, and D. Hilvert, "A photoinducible β-hairpin," *Journal of the American Chemical Society,* vol. 127, no. 9, pp. 2929-2936, 2005.
[20] R. Huang, Y. Wang, W. Qi, R. Su, and Z. He, "Temperature-induced reversible self-assembly of diphenylalanine peptide and the structural transition from organogel to crystalline nanowires," *Nanoscale research letters,* vol. 9, no. 1, p. 653, 2014.
[21] A. Dasgupta, J. H. Mondal, and D. Das, "Peptide hydrogels," *Rsc Advances,* vol. 3, no. 24, pp. 9117-9149, 2013.
[22] T. Otsuka, T. Maeda, and A. Hotta, "Effects of Salt Concentrations of the Aqueous Peptide-Amphiphile Solutions on the Sol–Gel Transitions, the Gelation Speed, and the Gel Characteristics," *The Journal of Physical Chemistry B,* vol. 118, no. 39, pp. 11537-11545, 2014.
[23] R. B. Merrifield, "Solid phase peptide synthesis. I. The synthesis of a tetrapeptide," *Journal of the American Chemical Society,* vol. 85, no. 14, pp. 2149-2154, 1963.
[24] H. Cui, M. J. Webber, and S. I. Stupp, "Self-assembly of peptide amphiphiles: From molecules to nanostructures to biomaterials," *Peptide Science,* vol. 94, no. 1, pp. 1-18, 2010.
[25] K. Hinterding, D. Alonso-Díaz, and H. Waldmann, "Organic synthesis and biological signal transduction," *Angewandte Chemie International Edition,* vol. 37, no. 6, pp. 688-749, 1998.
[26] D. W. Löwik and J. C. van Hest, "Peptide based amphiphiles," *Chemical Society Reviews,* vol. 33, no. 4, pp. 234-245, 2004.
[27] S. J. Singer and G. L. Nicolson, "The fluid mosaic model of the structure of cell membranes," *Science,* vol. 175, no. 4023, pp. 720-731, 1972.
[28] H. Lodish, A. Berk, S. L. Zipursky, P. Matsudaira, D. Baltimore, and J. Darnell, *Molecular cell biology*. Scientific American Books New York, 1995.
[29] A. Trent, R. Marullo, B. Lin, M. Black, and M. Tirrell, "Structural properties of soluble peptide amphiphile micelles," *Soft Matter,* vol. 7, no. 20, pp. 9572-9582, 2011.
[30] A. Dehsorkhi, V. Castelletto, and I. W. Hamley, "Self-assembling amphiphilic peptides," *Journal of Peptide Science,* vol. 20, no. 7, pp. 453-467, 2014.
[31] K. L. Niece *et al.*, "Modification of gelation kinetics in bioactive peptide amphiphiles," *Biomaterials,* vol. 29, no. 34, pp. 4501-4509, 2008.
[32] H. Cui, T. Muraoka, A. G. Cheetham, and S. I. Stupp, "Self-assembly of giant peptide nanobelts," *Nano letters,* vol. 9, no. 3, pp. 945-951, 2009
[33] S. Mura, J. Nicolas, and P. Couvreur, "Stimuli-responsive nanocarriers for drug delivery," *Nature materials,* vol. 12, no. 11, p. 991, 2013.
[34] J. D. Hartgerink, E. Beniash, and S. I. Stupp, "Self-assembly and mineralization of peptide-amphiphile nanofibers," *Science,* vol. 294, no. 5547, pp. 1684-1688, 2001.
[35] A. Tan, J. Rajadas, and A. M. Seifalian, "Biochemical engineering nerve conduits using peptide amphiphiles," *Journal of controlled release,* vol. 163, no. 3, pp. 342-352, 2012.
[36] X. Zhang and C. Wang, "Supramolecular amphiphiles," *Chemical Society Reviews,* vol. 40, no. 1, pp. 94-101, 2011.
[37] I. Hamley, "Self-assembly of amphiphilic peptides," *Soft Matter,* vol. 7, no. 9, pp. 4122-4138, 2011.
[38] M. Wei, Y. Gao, X. Li, and M. J. Serpe, "Stimuli-responsive polymers and their applications," *Polymer Chemistry,* vol. 8, no. 1, pp. 127-143, 2017.

[39] E. Cabane, X. Zhang, K. Langowska, C. G. Palivan, and W. Meier, "Stimuli-responsive polymers and their applications in nanomedicine," *Biointerphases,* vol. 7, no. 1-4, p. 9, 2012.

[40] K. Dutta, A. Alexandrov, H. Huang, and S. M. Pascal, "pH-induced folding of an apoptotic coiled coil," *Protein Science,* vol. 10, no. 12, pp. 2531-2540, 2001.

[41] L. A. Haines, K. Rajagopal, B. Ozbas, D. A. Salick, D. J. Pochan, and J. P. Schneider, "Light-activated hydrogel formation via the triggered folding and self-assembly of a designed peptide," *Journal of the American Chemical Society,* vol. 127, no. 48, pp. 17025-17029, 2005.

[42] E. Beniash, J. D. Hartgerink, H. Storrie, J. C. Stendahl, and S. I. Stupp, "Self-assembling peptide amphiphile nanofiber matrices for cell entrapment," *Acta biomaterialia,* vol. 1, no. 4, pp. 387-397, 2005.

[43] B. H. Jones *et al.*, "A multi-stimuli responsive, self-assembling, boronic acid dipeptide," *Chemical Communications,* vol. 51, no. 77, pp. 14532-14535, 2015.

[44] H. Matsui and B. Gologan, "Crystalline glycylglycine bolaamphiphile tubules and their pH-sensitive structural transformation," *The Journal of Physical Chemistry B,* vol. 104, no. 15, pp. 3383-3386, 2000.

[45] Z. Yang, G. Liang, L. Wang, and B. Xu, "Using a kinase/phosphatase switch to regulate a supramolecular hydrogel and forming the supramolecular hydrogel in vivo," *Journal of the American Chemical Society,* vol. 128, no. 9, pp. 3038-3043, 2006.

[46] Y. Zhang, H. Gu, Z. Yang, and B. Xu, "Supramolecular hydrogels respond to ligand−receptor interaction," *Journal of the American Chemical Society,* vol. 125, no. 45, pp. 13680-13681, 2003.

[47] D. G. Hall, "Structure, properties, and preparation of boronic acid derivatives. Overview of their reactions and applications," *Boronic acids: preparation and applications in organic synthesis and medicine,* vol. 1, pp. 1-99, 2006.

[48] J. N. Cambre and B. S. Sumerlin, "Biomedical applications of boronic acid polymers," *Polymer,* vol. 52, no. 21, pp. 4631-4643, 2011.

[49] G. F. Whyte, R. Vilar, and R. Woscholski, "Molecular recognition with boronic acids—applications in chemical biology," *Journal of chemical biology,* vol. 6, no. 4, pp. 161-174, 2013.

[50] Y. Li *et al.*, "Well-Defined, Reversible Boronate Crosslinked Nanocarriers for Targeted Drug Delivery in Response to Acidic pH Values and cis-Diols," *Angewandte chemie,* vol. 124, no. 12, pp. 2918-2923, 2012.

[51] M.-S. Steiner, A. Duerkop, and O. S. Wolfbeis, "Optical methods for sensing glucose," *Chemical Society Reviews,* vol. 40, no. 9, pp. 4805-4839, 2011.

[52] R. Nishiyabu, Y. Kubo, T. D. James, and J. S. Fossey, "Boronic acid building blocks: tools for sensing and separation," *Chemical Communications,* vol. 47, no. 4, pp. 1106-1123, 2011.

[53] X. Wu, Z. Li, X.-X. Chen, J. S. Fossey, T. D. James, and Y.-B. Jiang, "Selective sensing of saccharides using simple boronic acids and their aggregates," *Chemical Society Reviews,* vol. 42, no. 20, pp. 8032-8048, 2013.

[54] Y. Furikado *et al.*, "Universal reaction mechanism of boronic acids with diols in aqueous solution: kinetics and the basic concept of a conditional formation constant," *Chemistry-A European Journal,* vol. 20, no. 41, pp. 13194-13202, 2014.

[55] E. Watanabe *et al.*, "Relative kinetic reactivity of boronic acid and boronate ion towards Tiron, 2, 2'-biphenol, and propylene glycol," *Dalton Transactions,* vol. 42, no. 23, pp. 8446-8453, 2013.

[56] J. Yan, G. Springsteen, S. Deeter, and B. Wang, "The relationship among pK a, pH, and binding constants in the interactions between boronic acids and diols—it is not as simple as it appears," *Tetrahedron,* vol. 60, no. 49, pp. 11205-11209, 2004.

[57] H. R. Mulla, N. J. Agard, and A. Basu, "3-Methoxycarbonyl-5-nitrophenyl boronic acid: high affinity diol recognition at neutral pH," *Bioorganic & medicinal chemistry letters,* vol. 14, no. 1, pp. 25-27, 2004.

[58] M. Meiland, T. Heinze, W. Guenther, and T. Liebert, "Seven-membered ring boronates at trans-diol moieties of carbohydrates," *Tetrahedron Letters,* vol. 50, no. 4, pp. 469-472, 2009.

[59] C. Ke, H. Destecroix, M. P. Crump, and A. P. Davis, "A simple and accessible synthetic lectin for glucose recognition and sensing," *Nature chemistry,* vol. 4, no. 9, pp. 718-723, 2012.

[60] J. P. Lorand and J. O. EDWARDS, "Polyol complexes and structure of the benzeneboronate ion," *The Journal of Organic Chemistry,* vol. 24, no. 6, pp. 769-774, 1959.

[61] S. J. Angyal, "The composition of reducing sugars in solution," *Advances in carbohydrate chemistry and biochemistry,* vol. 42, pp. 15-68, 1984.

[62] S. J. Angyal, "The composition of reducing sugars in solution: Current aspects," *Advances in carbohydrate chemistry and biochemistry,* vol. 49, pp. 19-35, 1991.

[63] T. D. James, M. D. Phillips, and S. Shinkai, *Boronic acids in saccharide recognition*. Royal Society of Chemistry, 2006.

[64] Z.-A. Lin, J.-N. Zheng, F. Lin, L. Zhang, Z. Cai, and G.-N. Chen, "Synthesis of magnetic nanoparticles with immobilized aminophenylboronic acid for selective capture of glycoproteins," *Journal of Materials Chemistry,* vol. 21, no. 2, pp. 518-524, 2011.

[65] M. Winson, M. P. áPereira Morais, J. M. ávan den Elsen, and P. Jonathan, "Dye displacement assay for saccharide detection with boronate hydrogels," *Chemical Communications,* no. 5, pp. 532-534, 2009.

[66] G. Springsteen and B. Wang, "Alizarin Red S. as a general optical reporter for studying the binding of boronic acids with carbohydrates," *Chemical Communications,* no. 17, pp. 1608-1609, 2001.

[67] G. Springsteen and B. Wang, "A detailed examination of boronic acid–diol complexation," *Tetrahedron,* vol. 58, no. 26, pp. 5291-5300, 2002.

[68] Y. Kubo, T. Ishida, A. Kobayashi, and T. D. James, "Fluorescent alizarin–phenylboronic acid ensembles: design of self-organized molecular sensors for metal ions and anions," *Journal of Materials Chemistry,* vol. 15, no. 27-28, pp. 2889-2895, 2005.

[69] W. Scarano, H. Lui, and M. H. Stenzel "Boronic acid ester with dopamine as a tool for bioconjugation and for visualization of cell apoptosis," *Chemical Communications,* vol. 50 no. 48 pp. 6390-6393, 2014.

[70] Y. Kan, E. W. Danner, J. N. Israelachvili, Y. Chen, and J. H. Waite, "Boronate complex formation with Dopa containing mussel adhesive protein retards pH-induced oxidation and enables adhesion to mica," *PloS one,* vol. 9, no. 10, p. e108869, 2014.

[71] B. P. Lee, P. B. Messersmith, J. N. Israelachvili, and J. H. Waite, "Mussel-inspired adhesives and coatings," *Annual review of materials research,* vol. 41, pp. 99-132, 2011.

[72] J. Sedó, J. Saiz-Poseu, F. Busqué, and D. Ruiz-Molina, "Catechol-Based Biomimetic Functional Materials," *Advanced Materials,* vol. 25, no. 5, pp. 653-701, 2013.

[73] J. Yu, W. Wei, E. Danner, R. K. Ashley, J. N. Israelachvili, and J. H. Waite, "Mussel protein adhesion depends on interprotein thiol-mediated redox modulation," *Nature chemical biology,* vol. 7, no. 9, pp. 588-590, 2011.

[74] E. W. Danner, Y. Kan, M. U. Hammer, J. N. Israelachvili, and J. H. Waite, "Adhesion of mussel foot protein Mefp-5 to mica: an underwater superglue," *Biochemistry,* vol. 51, no. 33, pp. 6511-6518, 2012.

[75] M. S. Menyo, C. J. Hawker, and J. H. Waite, "Versatile tuning of supramolecular hydrogels through metal complexation of oxidation-resistant catechol-inspired ligands," *Soft Matter,* vol. 9, no. 43, pp. 10314-10323, 2013.

[76] T. Ptak, P. Młynarz, A. Dobosz, A. Rydzewska, and M. Prokopowicz, "Potentiometric and NMR complexation studies of phenylboronic acid PBA and its aminophosphonate analog with selected catecholamines," *Journal of Molecular Structure,* vol. 1040, pp. 59-64, 2013.

[77] H. Ueno, T. Iwata, N. Koshiba, D. Takahashi, and K. Toshima, "Design, synthesis and evaluation of a boronic acid based artificial receptor for l-DOPA in aqueous media," *Chemical Communications,* vol. 49, no. 88, pp. 10403-10405, 2013.

[78] Z. Wu, X. Yang, W. Xu, B. Wang, and H. Fang, "A new boronic acid-based fluorescent sensor for L-dihydroxy-phenylalanine," *Drug discoveries & therapeutics,* vol. 6, no. 5, pp. 238-241, 2012.

[79] V. Yesilyurt, M. J. Webber, E. A. Appel, C. Godwin, R. Langer, and D. G. Anderson, "Injectable Self-Healing Glucose-Responsive Hydrogels with pH-Regulated Mechanical Properties," *Advanced Materials,* vol. 28, no. 1, pp. 86-91, 2016.

[80] K. Lacina, P. Skládal, and T. D. James, "Boronic acids for sensing and other applications-a mini-review of papers published in 2013," *Chemistry Central Journal,* vol. 8, no. 1, p. 60, 2014.

[81] Z. Wei *et al.*, "Self-healing gels based on constitutional dynamic chemistry and their potential applications," *Chemical Society Reviews,* vol. 43, no. 23, pp. 8114-8131, 2014.

[82] C. C. Deng, W. L. Brooks, K. A. Abboud, and B. S. Sumerlin, "Boronic acid-based hydrogels undergo self-healing at neutral and acidic pH," *ACS Macro Letters,* vol. 4, no. 2, pp. 220-224, 2015.

[83] C. Alvarez-Lorenzo and A. Concheiro, *Smart materials for drug delivery*. Royal Society of Chemistry, 2013.

[84] D. Roy, J. N. Cambre, and B. S. Sumerlin, "Future perspectives and recent advances in stimuli-responsive materials," *Progress in Polymer Science,* vol. 35, no. 1, pp. 278-301, 2010.

[85] K. Kataoka, H. Miyazaki, M. Bunya, T. Okano, and Y. Sakurai, "Totally synthetic polymer gels responding to external glucose concentration: their preparation and application to on− off regulation of insulin release," *Journal of the American Chemical Society,* vol. 120, no. 48, pp. 12694-12695, 1998.

[86] Y. Zhang, Y. Guan, and S. Zhou, "Synthesis and volume phase transitions of glucose-sensitive microgels," *Biomacromolecules,* vol. 7, no. 11, pp. 3196-3201, 2006.

[87] N. A. Siddiqui, N. Billa, and C. J. Roberts, "Multiboronic acid-conjugated chitosan scaffolds with glucose selectivity to insulin release," *Journal of Biomaterials Science, Polymer Edition,* vol. 28, no. 8, pp. 781-793, 2017.

[88] H. Liu *et al.*, "Dual-responsive surfaces modified with phenylboronic acid-containing polymer brush to reversibly capture and release cancer cells," *Journal of the American Chemical Society,* vol. 135, no. 20, pp. 7603-7609, 2013.

[89] K. A. Sarosiek *et al.*, "Efficacy of bortezomib in a direct xenograft model of primary effusion lymphoma," *Proceedings of the National Academy of Sciences,* vol. 107, no. 29, pp. 13069-13074, 2010.

[90] M. Wang, Y. Wang, K. Hu, N. Shao, and Y. Cheng, "Tumor extracellular acidity activated “off–on” release of bortezomib from a biocompatible dendrimer," *Biomaterials science,* vol. 3, no. 3, pp. 480-489, 2015.

[91] A. Swami *et al.*, "Engineered nanomedicine for myeloma and bone microenvironment targeting," *Proceedings of the National Academy of Sciences,* vol. 111, no. 28, pp. 10287-10292, 2014.

[92] J. Shen *et al.*, "The use of hollow mesoporous silica nanospheres to encapsulate bortezomib and improve efficacy for non-small cell lung cancer therapy," *Biomaterials,* vol. 35, no. 1, pp. 316-326, 2014.

[93] J. Su, F. Chen, V. L. Cryns, and P. B. Messersmith, "Catechol polymers for pH-responsive, targeted drug delivery to cancer cells," *Journal of the American Chemical Society,* vol. 133, no. 31, pp. 11850-11853, 2011.

[94] P. Shen and Y. Xia, "Synthesis-modification integration: one-step fabrication of boronic acid functionalized carbon dots for fluorescent blood sugar sensing," *Analytical chemistry,* vol. 86, no. 11, pp. 5323-5329, 2014.

[95] N. Ogata, S. W. Kim, J. Feijen, and T. Okano, *Advanced biomaterials in biomedical engineering and drug delivery systems*. Springer Science & Business Media, 2012.

[96] T. M.Allen and P. R.Cullis,"Liposomal drug delivery systems: from concept to clinical applications," *Advanced drug delivery reviews,* vol. 65, no. 1, pp. 36-48, 2013.

[97] Y. Yin and D. Talapin, "The chemistry of functional nanomaterials," *Chemical Society Reviews,* vol. 42, no. 7, pp. 2484-2487, 2013.